Article

Diverse Stereocontrol Effects Induced by Weakly Coordinating Anions. Stereospecific Olefin Polymerization Pathways at Archetypal *C*- and *C*-Symmetric Metallocenium Catalysts Using Mono- and Polynuclear Halo-perfluoroarylmetalates as Cocatalysts

John A. S. Roberts, Ming-Chou Chen, Afif M. Seyam, Liting Li, Cristiano Zuccaccia, Nicholas G. Stahl, and Tobin J. Marks

J. Am. Chem. Soc., **2007**, 129 (42), 12713-12733• DOI: 10.1021/ja0680360 • Publication Date (Web): 02 October 2007

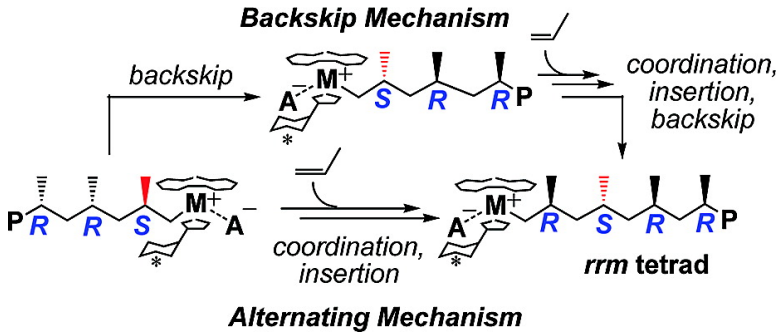

More About This Article

Additional resources and features associated with this article are available within the HTML version:

- Supporting Information
- Links to the 4 articles that cite this article, as of the time of this article download
- Access to high resolution figures
- Links to articles and content related to this article
- Copyright permission to reproduce figures and/or text from this article

View the Full Text HTML

J|A|C|S
ARTICLES
Published on Web 10/02/2007

Diverse Stereocontrol Effects Induced by Weakly Coordinating Anions. Stereospecific Olefin Polymerization Pathways at Archetypal C_s- and C_1-Symmetric Metallocenium Catalysts Using Mono- and Polynuclear Halo-perfluoroarylmetalates as Cocatalysts

John A. S. Roberts, Ming-Chou Chen, Afif M. Seyam, Liting Li, Cristiano Zuccaccia, Nicholas G. Stahl, and Tobin J. Marks*

Contribution from the Department of Chemistry, Northwestern University, Evanston, Illinois 60208-3113

Received November 15, 2006; E-mail: t-marks@northwestern.edu

Abstract: Counteranion effects on propylene polymerization rates and stereoselectivities are compared using C_s-symmetric $Me_2C(Cp)(Flu)ZrMe_2$ (**1**; Cp = C_5H_4,η^5-cyclopentadienyl; Flu = $C_{13}H_8$, η^5-fluorenyl) and C_1-symmetric $Me_2Si(OHF)(CpR^*)ZrMe_2$ (**2**; OHF = $C_{13}H_{16}$, η^5-octahydrofluorenyl; CpR* = η^5-3-(−)-menthylcyclopentadienyl) precatalysts activated with the mononuclear and polynuclear perfluoroarylborate, -aluminate, and -gallate cocatalysts/activators $B(C_6F_5)_3$ (**3**), $B(o\text{-}C_6F_5C_6F_4)_3$ (**4**), $Al(C_6F_5)_3$ (**5**), $Ph_3C^+B(C_6F_5)_4^-$ (**6**) $Ph_3C^+FAl(o\text{-}C_6F_5C_6F_4)_3^-$ (**7**), $Ga(C_6F_5)_3$ (**8**), and recently reported mono- and polymetallic trityl perfluoroarylhalometalates $Ph_3C^+FB(C_6F_5)_3^-$ (**9**), $Ph_3C^+FB(o\text{-}C_6F_5C_6F_4)_3^-$ (**10**), $(Ph_3C^+)_xF_x[Al(C_6F_5)_3]_y^{x-}$ (x = 1, y = 1, **11**; x = 1, y = 2, **12**; x = 2, y = 3, **13**), $Ph_3C^+(C_6F_5)_3AlFAl(o\text{-}C_6F_5C_6F_4)_3^-$ (**14**), $Ph_3C^+XAl(C_6F_5)_3^-$ (X = Cl, **15**; X = Br, **16**), and $Ph_3C^+F[Ga(C_6F_5)_3]_2^-$ (**17**). Temperature, propylene concentration, and solvent polarity dependence are surveyed in polymerizations catalyzed by **1** activated with cocatalysts **3**−**16** and with a 1:2 ratio of Ph_3CCl and **5**, and with a 1:2 ratio of Ph_3CBr and **5**, and by **2** activated with **3**, **6**, **7**, **12**, and **14**. Remarkable stereocontrol with high activities is observed for **1** + **12** and **1** + **14**. Polypropylene samples produced using C_1-symmetric precatalyst **2** are subjected to microstructural analyses using stochastic models describing the relative contributions of enantiofacial misinsertion and backskip processes. A powerful technique is introduced for calculating interparametric correlation matrices for these nonlinear stochastic models. The collected results significantly extend what is known about ion-pairing effects in the case of C_s-symmetric precatalyst **1** and allow these findings to be applied to the case of C_1-symmetric precatalyst **2** as an agent of isospecific propylene polymerization.

Introduction

A new understanding of the significance of ion-pairing interactions in metallocene-based olefin polymerization catalyst systems (**A**, produced via metallocene alkide abstraction by neutral or ionic organometalloid activators; eq 1) has emerged from recent studies of catalyst system ion-pairing dynamics.[1−4]

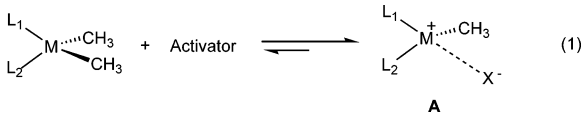

(1)

A

Importantly, it is evident that (a) in low-ϵ media at catalyst concentrations typical for olefin polymerization reactions, these catalyst systems exist as stereochemically mobile 1:1 contact ion-pairs and exhibit varying modes and strengths of cation−anion interaction,[2,5,6] and (b) during polymerization reactions, the rates of a host of competing processes, including chain-migratory insertion (chain propagation), various stereodefect production and polymer chain termination processes, and even catalyst deactivation, are all profoundly anion-dependent, with strong correlations between the rates of processes occurring during polymerization and active catalyst ion-pairing strength as assayed by *ex situ* solution-phase spectroscopic studies of the catalyst systems.[7] These findings suggest that polymerization-significant ion-pairing must persist under polymerization conditions and that the anion-derived effects on activity, stereoregulation, and chain release are deeply rooted in ion-pairing dynamics. This stands to reason: in asymmetric catalysis, the influence of catalyst ancillary moieties on transition-state energies generally increases with increasing proximity to the catalyst active site; in the case of ion-paired polymerization catalysts, the counteranion can compete for occupancy of the active site with incoming monomer. The emerging picture then is one in which the interplay between counteranion, cation−

(1) For recent reviews of single-site olefin polymerization, see: (a) Marks, T. J. Ed. Special Feature on Polymerization, *Proc. Natl. Acad. Sci. U.S.A.* **2006**, *103*, 15288. Also therein: Li, H.; Marks, T. J. *Proc. Natl. Acad. Sci. U.S.A.* **2006**, *103*, 15295−15302. (b) Gibson, V. C.; Spitzmesser, S. K. *Chem. Rev.* **2003**, *103*, 283−315. (c) Pédeutour, J.-N.; Radhakrishnan, K.; Cramail, H.; Deffieux, A. *Macromol. Rapid Commun.* **2001**, *22*, 1095−1123. (d) Chen, Y.-X.; Marks, T. J. *Chem. Rev.* **2000**, *100*, 1391−1434. (e) Gladysz, J. A., Ed. *Chem. Rev.* **2000**, *100*, 1167−1682. (f) Marks, T. J., Stevens, J. C., Eds. *Top. Catal.* **1999**, *7*, 1−208. (g) Britovsek, G. J. P.; Gibson, V. C.; Wass, D. F. *Angew. Chem., Int. Ed.* **1999**, *38*, 428−447.

polymeryl moiety, and incoming monomer dictates the relative rates of the various processes occurring at the catalytic center during the polymerization process. Cocatalyst/anion effects thus have a direct influence on catalyst performance and product polymer properties such as stereo- and regioregularity and molar mass.

Major advances in the study of metallocene-mediated olefin polymerization have followed from the discovery and development of new activator/cocatalyst classes having distinctive properties: alkylaluminoxanes (e.g., MAO and MMAO),[8] tris(perfluorophenyl)borane ($B(C_6F_5)_3$, **3**)[3] and related perfluoroarylboranes,[9] ammonium or trityl salts of $B(C_6F_5)_4^-$ [4] and related perfluoroarylborates,[10] perfluoroarylalanes (e.g., $Al(C_6F_5)_3$, **7**),[11] and perfluoroaryl fluoroaluminate salts.[12] We recently reported new classes of mononuclear and polynuclear fluoro- and perfluoroarylborate, -aluminate, and -gallate weakly coordinating anions and cocatalysts having one or more metalloid-bound halogen atoms in $[M-X]^-$, $[M-X-M]^-$, and $[M-X-M-X-M]^{2-}$ bonding configurations,[13,14] with the synthetic and metallocene activation chemistry of these species typically involving formation or cleavage of these metalloid−halogen bonds. These more sterically encumbered and charge-dispersing cocatalysts afford thermally robust active catalyst systems that can produce highly stereoregular polypropylenes with very high polymerization activities.

Herein we compare and contrast the propylene polymerization behavior of active catalyst systems derived from cocatalysts $Al(C_6F_5)_3$ (**5**), *in situ*-generated $Ga(C_6F_5)_3$ (**8**), and the new trityl perfluoroaryl fluoroborates $Ph_3C^+FB(C_6F_5)_3^-$ (**9**)[15] and $Ph_3C^+FB(o\text{-}C_6F_5C_6F_4)_3^-$ (**10**), a homologous series of mono- and polynuclear perfluoroaryl fluoroaluminates $(Ph_3C^+)_xF_x[Al(C_6F_5)_3]_y^{x-}$ ($x = 1$, $y = 1$, **11**; $x = 1$, $y = 2$, **12**; $x = 2$, $y = 3$, **13**),[16,17] $Ph_3C^+(C_6F_5)_3AlFAl(o\text{-}C_6F_5C_6F_4)_3^-$ (**14**), the haloaluminates $Ph_3C^+XAl(C_6F_5)_3^-$ (X = Cl, **15**; X = Br, **16**), and binuclear fluorine-bridged gallate $Ph_3C^+F[Ga(C_6F_5)_3]_2^-$ (**17**),[18] in combination with archetypal C_s-symmetric precatalyst $Me_2C(Cp)(Flu)ZrMe_2$ (**1**; Cp = C_5H_4, η^5-cyclopentadienyl; Flu = $C_{13}H_8$, η^5-fluorenyl) and also with the C_1-symmetric precatalyst $Me_2Si(OHF)(CpR^*)ZrMe_2$ (**2**; OHF = $C_{13}H_{16}$, η^5-octahydrofluorenyl; CpR* = η^5-3-(−)-menthylcyclopentadienyl; structures of precatalysts **1** and **2** and cocatalysts **3**−**17** are depicted in Scheme 1). We also describe polymerization results obtained using precatalyst **1** activated with cocatalyst preparations in which $Al(C_6F_5)_3$ (**5**) is combined with the reagent Ph_3CCl in a 2:1 ratio ("$Ph_3C^+Cl[Al(C_6F_5)_3]_2^-$"), and in which **5** is combined with Ph_3CBr in a 2:1 ratio ("$Ph_3C^+Br[Al(C_6F_5)_3]_2^-$").[19]

Our detailed mechanistic picture of counteranion effects in syndiospecific propylene polymerization derives in part from polypropylene microstructural analysis,[1d] a quantitative treatment in which the relative abundances of certain defects in an otherwise stereoregular polymer backbone are modeled according to a collection of proposed stereodefect-producing mechanisms, the relative rates of which can then be estimated. Application of this this approach to catalytic systems based on C_1-symmetric precatalyst $Me_2Si(OHF)(CpR^*)ZrMe_2$ (**2**) plus the present cocatalysts should, in principle, allow a similar level of detail to be achieved. To this end, the substantially isotactic polypropylene samples produced using C_1-symmetric precatalyst **2** are subjected to microstructural analyses using a standard parametrization describing the relative contributions of proposed enantiofacial misinsertion and backskip mechanisms (*vide infra*). This model is presented along with a series of submodels based on some reasonable simplifying assumptions and a powerful new technique for calculating matrices of correlation coefficients

(2) For recent cocatalyst studies, see: (a) Busico, V.; Cipullo, R.; Cutillo, F.; Vacatello, M.; Castelli, V. V. *Macromolecules* **2003**, *36*, 4258−4261. (b) Mohammed, M.; Nele, M.; Al-Humydi, A.; Xin, S.; Stapleton, R. A.; Collins, S. *J. Am. Chem. Soc.* **2003**, *125*, 7930−7941. (c) Abramo, G. P.; Li, L.; Marks, T. J. *J. Am. Chem. Soc.* **2002**, *124*, 13966−13967. (d) Li, L.; Metz, M. V.; Li, H.; Chen, M. C.; Marks, T. J. *J. Am. Chem. Soc.* **2002**, *124*, 12725−12741. (e) Metz, M. V.; Schwartz, D. J.; Stern, C. L.; Marks, T. J.; Nickias, P. N. *Organometallics* **2002**, *21*, 4159−4168. (f) Metz, M. V.; Sun, Y. M.; Stern, C. L.; Marks, T. J. *Organometallics* **2002**, *21*, 3691−3702. (g) Wilmes, G. M.; Polse, J. L.; Waymouth, R. M. *Macromolecules* **2002**, *35*, 6766−6772. (h) Lancaster, S. J.; Rodriguez, A.; Lara-Sanchez, A.; Hannant, M. D.; Walker, D. A.; Hughes, D. H.; Bochmann, M. *Organometallics* **2002**, *21*, 451−453. (i) Rodriguez, G.; Brant, P. *Organometallics* **2001**, *20*, 2417−2420. (j) Kaul, F. A. R.; Puchta, G. T.; Schneider, H.; Grosche, M.; Mihalios, D.; Herrmann, W. A. *J. Organometal. Chem.* **2001**, *621*, 177−183. (k) Chen, Y. X.; Kruper, W. J.; Roof, G.; Wilson, D. R. *J. Am. Chem. Soc.* **2001**, *123*, 745−746. (l) Zhou, J.; Lancaster, S. J.; Walker, D. A.; Beck, S.; Thornton-Pett, M.; Bochmann, M. *J. Am. Chem. Soc.* **2001**, *123*, 223−237. (m) Kehr, G.; Roesmann, R.; Fröhlich, R.; Holst, C.; Erker, G. *Eur. I. Inorg. Chem.* **2001**, 535−538. (n) Mager, M.; Becke, S.; Windisch, H.; Denninger, U. *Angew. Chem., Int. Ed.* **2001**, *40*, 1898−1902. (o) Al-Humydi, A.; Garrison, J. C.; Youngs, W. J.; Collins, S. *Organometallics* **2005**, *24*, 193−196. (p) Lancaster, S. J.; Bochmann, M. *J. Organomet. Chem.* **2002**, *654*, 221−223.

(3) (a) Yang, X.; Stern, C. L.; Marks, T. J. *J. Am. Chem. Soc.* **1994**, *116*, 10015−10031. (b) Yang, X.; Stern, C. L.; Marks, T. J. *J. Am. Chem. Soc.* **1991**, *113*, 3623−3625.

(4) (a) Chien, J. C. W.; Tsai, W.-M.; Rausch, M. D. *J. Am. Chem. Soc*. **1991**, *113*, 8570−8571. (b) Yang, X.; Stern, C. L.; Marks, T. J. *Organometallics* **1991**, *10*, 840−842. (c) Ewen, J. A.; Elder, M. J. Eur. Pat. Appl. 426637, 1991; *Chem. Abstr*. **1991**, *115*, 136987c, 136988d.

(5) (a) Stahl, N. G.; Zuccaccia, C.; Jensen, T. R.; Marks, T. J. *J. Am. Chem. Soc.* **2003**, *125*, 5256−5257. (b) Stahl, N. G.; Marks, T. J.; Macchioni, A.; Zuccaccia, C. Presented in part at the 222nd ACS National Meeting, Chicago, IL, August 2001; Abstract INORG 407.

(6) Song, F.; Lancaster, S. J.; Cannon, R. D.; Schormann, M.; Humphrey, S. M.; Zuccaccia, C.; Macchioni, A.; Bochmann, M. *Organometallics* **2005**, *24*, 1315−1328.

(7) Chen, M. C.; Roberts, J. A. S.; Marks, T. J. *J. Am. Chem. Soc.* **2004**, *126*, 4605−4625.

(8) (a) Sinn, H.; Kaminsky, W. *Adv. Organomet. Chem*. **1980**, *18*, 99−149. (b) Sinn, H.; Kaminsky, W.; Vollmer, H.-J.; Woldt, R. *Angew. Chem., Int. Ed. Engl*. **1980**, *19*, 390−392.

(9) (a) Li, L.; Stern, C. L.; Marks, T. J. *Organometallics* **2000**, *19*, 3332−3337. (b) Li, L.; Marks, T. J. *Organometallics* **1998**, *17*, 3996−4003. (c) Chen, Y.-X.; Stern, C. L.; Yang, S.; Marks, T. J. *J. Am. Chem. Soc.* **1996**, *118*, 12451−12452. (d) Also see refs 2c−e. (e) For a recent chelating borane review, see: Piers, W. E.; Irvine, G. J.; Williams, V. C. *Eur. J. Inorg. Chem.* **2000**, 2131−2142.

(10) For related fluorinated tetraarylborates, see: (a) refs 2h−j,l. (b) Jia, L.; Yang, X.; Stern, C. L.; Marks, T. J. *Organometallics* **1997**, *16*, 842−857. (c) Jia, L.; Yang, X.; Ishihara, A.; Marks, T. J. *Organometallics* **1995**, *14*, 3135−3137.

(11) (a) Reference 2f. (b) Bochmann, M.; Sarsfield, M. J. *Organometallics* **1998**, *17*, 5908−5912. (c) Biagini, P.; Lugli, G.; Abis, L.; Andreussi, P. U.S. Patent 5,602,269, 1997.

(12) (a) Chen, Y.-X.; Metz, M. V.; Li, L.; Stern, C. L.; Marks, T. J. *J. Am. Chem. Soc.* **1998**, *120*, 6287−6305. (b) Chen, Y.-X.; Stern, C. L.; Marks, T. J. *J. Am. Chem. Soc.* **1997**, *119*, 2582−2583. (c) Elder, M. J.; Ewen, J. A. Eur. Pat. Appl. EP 573,403, 1993; *Chem. Abstr*. **1994**, *121*, 0207d. (d) Also ref 2p.

(13) Chen, M. -C.; Roberts, J. A. S.; Marks, T. J. *Organometallics* **2004**, *23*, 932−935.

(14) Syntheses and characterization of the present series of cocatalysts, and details of their stoichiometric reaction with metallocene **15**, are presented in a separate report: Chen, M.-C.; Roberts, J. A. S.; Seyam, A. M.; Li, L.; Zuccaccia, C.; Stahl, N. G.; Marks, T. J. *Organometallics* **2006**, *25*, 2833−2850.

(15) A similar fluoroborate, $Li^+[FB(C_6F_5)_3]^-$, has been claimed previously. See Klemann, L. P.; Newman, G. H.; Stogryn, E. L. U.S. Patent 4139681, 1979.

(16) For the first structural study of a fluoro-bridged organoaluminum complex, $K^+[(Et)_3Al\text{-}F\text{-}Al(Et)_3]^-$, with F−Al = 1.80(6) Å, see: Natta, G.; Allegra, G.; Perego, G.; Zambelli, A. *J. Am. Chem. Soc.* **1961**, *83*, 5033−5033.

(17) A similar M−F−M−F−M arrangement is seen in a Bi system. For a recent review of metal fluorides, see: Roesky, H. W.; Haiduc, I. *J. Chem. Soc., Dalton Trans.* **1999**, 2249−2264.

(18) For recent examples of organogallium−F complexes, see: (a) Werner, B.; Kräuter, T.; Neumüller, B. *Organometallics* **1996**, *15*, 3746−3751. (b) See ref 17a for examples of nonlinear fluoro-bridged Ga complexes. (c) Kräuter, T.; Neumuller, B. *Z. Anorg. Allg. Chem.* **1995**, *621*, 597−606.

(19) These latter cocatalyst preparations do not contain isolable molecular species but do produce polymerization-active catalyst systems when combined with metallocene precatalyst **1**.

Scheme 1. Chemical Structures, Compounds **1**−**17**

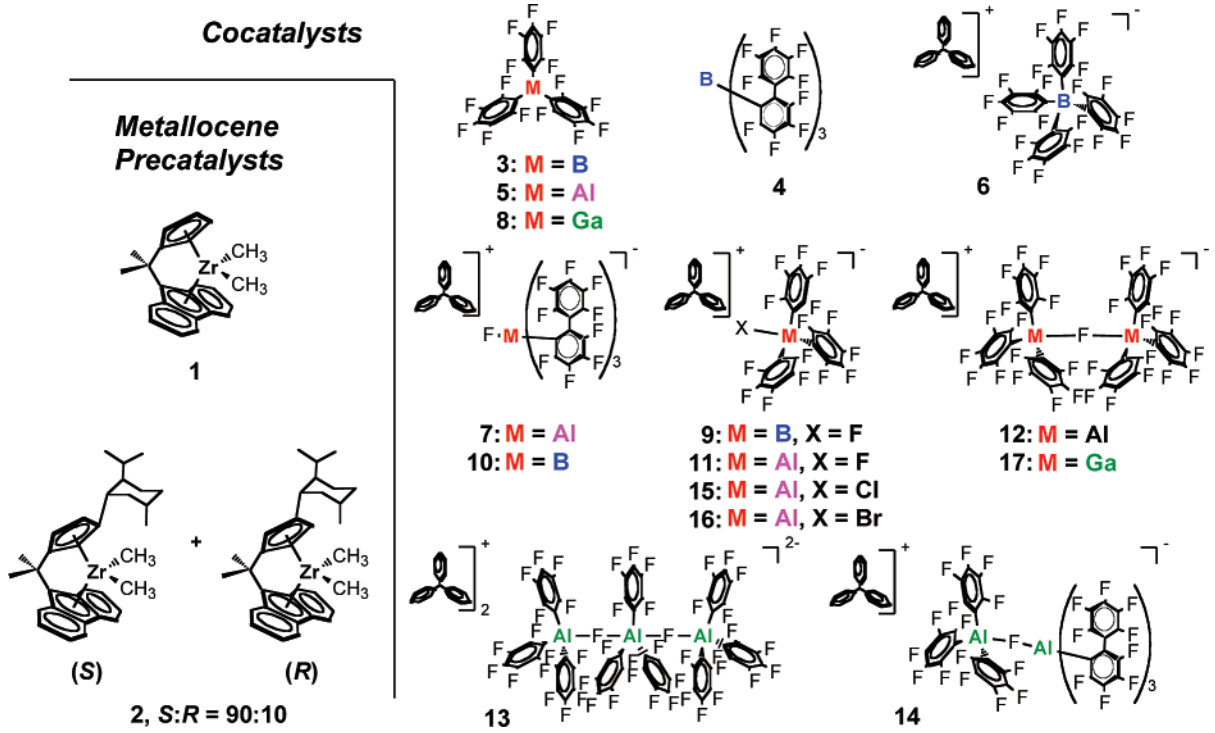

among the parameters of these nonlinear stochastic models. This particular analysis affords a clear picture of the strength of the stochastic approach as applied in the case of isospecific propylene polymerization. While the level of detail ascribable to the microstructural analysis of the present isotactic polypropylenes is found to be reduced in comparison to the syndiotactic case, observations on the overall stereoregularity of polymers produced using C_1-symmetric precatalyst **2** plus the present cocatalysts are consistent with the hypothesis demonstrated using C_s-symmetric precatalyst **1**, that ion-pairing strength is a key factor in determining the relative rates of individual processes available during polymerization.

Perfluoroarylmetalate complexes **9**−**16** are accessed by combining trityl halides with known neutral and ionic perfluoroaryl complexes of boron, aluminum, and gallium in varying stoichiometries. In a previous report,[14] we discussed the syntheses, solid-state structural features, and solution structural/dynamic features of these new cocatalysts and described the products generated in their reactions with metallocene **1**. In the present series of polymerization experiments, active catalyst systems are prepared by combining the C_s- or C_1-symmetric preactalyst and cocatalyst of choice and are used as described in the Experimental Section. We represent the catalyst system prepared by combining, for example, precatalyst **1** and cocatalyst **14** simply as "**1** + **14**". This serves to distinguish these preparations—often mixtures—from individual ion-pair complexes (isolable in certain cases by fractional recrystallization and identifiable as discrete species in the NMR spectra of certain catalyst-cocatalyst reaction mixtures).[7,14] Individual ion-pair complexes are referred to in the discussion using unique compound numbers **20**−**24**.

Catalyst systems generated using the present new polynuclear perfluoroaryl cocatalysts generally exhibit greater polymerization stereoregulation *and* higher polymerization rates than systems employing their mononuclear analogues, these differences being quite large in certain cases. As with the mononuclear systems, trends in polymer stereoregularity, the abundances of specific stereodefects, polymerization activity, and polymer molar mass are all found to be strongly cocatalyst-dependent. In general, *polynuclear* catalyst systems lacking a bridging μ-Me or μ-F cation−anion contact show substantially enhanced rates for both monomer enchainment and stereodefect-introducing reorganizations and misinsertions. These findings are discussed in detail, with special attention paid to systems in which both high activity and precise stereoregulation are obtained.

Experimental Section

Materials and Methods. All manipulations of air-sensitive materials were performed with rigorous exclusion of oxygen and moisture in flamed Schlenk-type glassware on a dual-manifold Schlenk line or interfaced to a high-vacuum line (10^{-6} Torr), or in an N_2-filled Vacuum Atmospheres or MBraun glovebox with a high capacity recirculator (<1 ppm O_2). Argon (Matheson, prepurified) and propylene (Matheson, polymerization grade) were purified by passage through a supported MnO-packed oxygen removal column and a column packed with activated Davidson 4-A molecular sieves. Hydrocarbon solvents (toluene and pentane) were distilled under nitrogen from Na/benzophenone ketyl or passed through columns packed with molecular seives and supported Cu(0) deoxygenating agent. These solvents were subsequently stored under vacuum over Na/K alloy in Teflon-valved bulbs and distilled on a high-vacuum line immediately prior to use. Deuterated solvents were obtained from Cambridge Isotope Laboratories (all ≥99 atom % D), freeze−pump−thaw degassed, dried over Na/K alloy, and stored in resealable flasks. Other non-halogenated solvents were dried over Na/K alloy, and halogenated solvents were distilled from CaH_2. $Me_2C(Cp)(Flu)ZrMe_2$ (**1**; Cp = C_5H_4, η^5-cyclopentadienyl; Flu = $C_{13}H_8$, η^5-fluorenyl),[20] $Me_2Si(OHF)(CpR^*)ZrMe_2$ (**2**; OHF = $C_{13}H_{16}$, η^5-octahydrofluorenyl; CpR* = η^5-3-(−)-menthylcyclopentadienyl, R* =

(20) (a) Razavi, A.; Thewalt, U. *J. Organomet. Chem.* **1993**, *445*, 111−114. (b) Razavi, A.; Ferrara, J. *J. Organomet. Chem.* **1992**, *435*, 299−310.

(1*R*,2*S*,5*R*)-*trans*-5-methyl-*cis*-2-(2-propyl)cyclohexyl ((−)-menthyl)),[21] $B(C_6F_5)_3$ (**3**),[22] $B(o\text{-}C_6F_5C_6F_4)_3$ (**4**),[9c] $Al(C_6F_5)_3\cdot 0.5(C_7H_8)$ (**5**),[23] $Ph_3C^+B(C_6F_5)_4^-$ (**6**),[24] and $Ph_3C^+FAl(o\text{-}C_6F_5C_6F_4)_3^-$ (**7**)[12a] were prepared according to literature procedures. $Ga(C_6F_5)_3$ (**8**) was generated *in situ* as described in refs 13 and 14. $Ph_3C^+FB(C_6F_5)_3^-$ (**9**), $Ph_3C^+FB(o\text{-}C_6F_5C_6F_4)_3^-$ (**10**), $(Ph_3C^+)_xF_x[Al(C_6F_5)_3]_y^{x-}$ ($x = 1$, $y = 1$, **11**; $x = 1$, $y = 2$, **12**; $x = 2$, $y = 3$, **13**), $Ph_3C^+(C_6F_5)_3AlFAl(o\text{-}C_6F_5C_6F_4)_3^-$ (**14**), $Ph_3C^+F[Ga(C_6F_5)_3]_2^-$ (**17**), and $Ph_3C^+XAl(C_6F_5)_3^-$ (X = Cl, **15**; X = Br, **16**) were prepared as described in refs 13 and 14. Trityl chloride (Ph_3CCl; Aldrich, 98%) was used as received.

Physical and Analytical Measurements. NMR spectra were recorded on Varian ^{UNITY}Inova-500 (FT, 500 MHz, ^1H; 125 MHz, ^{13}C), ^{UNITY}Inova-400 (FT, 400 MHz, ^1H; 100 MHz, ^{13}C), and Mercury-400 (FT 400 MHz, ^1H; 100 MHz, ^{13}C; 377 MHz, ^{19}F) instruments. Chemical shifts for ^1H and ^{13}C spectra were referenced using internal solvent resonances and are reported relative to tetramethylsilane. For ^{13}C NMR homopolymer microstructure analyses, either 300−400 mg polymer samples were dissolved in 4 mL of $C_2D_2Cl_4$ by heating with a heat gun in 10 mm NMR tubes, or 50−80 mg polymer samples were dissolved in 0.7 mL of $C_2D_2Cl_4$ in 5 mm NMR tubes. Samples thus prepared were transferred to the NMR spectrometer with the probehead at 125 °C, and the probehead and sample were allowed to equilibrate for 10 min. A 2.0 s acquisition time was used, with a pulse delay of 6.0 s. A total of 4000−6000 transients were accumulated for each spectrum. Pentad signals were assigned according to literature criteria.[25] Polymer melting temperatures were measured by differential scanning calorimetry (DSC 2920, TA Instruments, Inc.) from the second scan, with a heating rate of 10 °C/min. Gel permeation chromatographic (GPC) analyses of polymer samples were performed at the Dow Chemical Co., Chemical Sciences Catalysis Laboratory, Midland, MI, on a Waters Alliance GPCV 2000 high-temperature instrument. For each run, a polystyrene/polypropylene universal calibration was carried out using polystyrene standards.

Propylene Polymerization Experiments. Propylene polymerizations were carried out in a 350 mL heavy-wall glass pressure reactor (Chemglass Co., maximum pressure, 10 atm) equipped with a septum port, a large stir bar (stirring at 1000 rpm) to minimize mass transfer effects,[26] and an internal thermocouple probe (OMEGA Type K) to monitor possible exotherm effects[2d] and connected to a high-pressure manifold equipped with a gas inlet, diaphragm capacitance pressure gauge (0−200 psi), and gas outlet.[7] ***CAUTION: All of these procedures should be performed behind a blast shield.*** In a typical procedure, in the glovebox, the reactor was charged with dry toluene (50 mL) and the apparatus was assembled, removed, and then connected to the high-pressure manifold. Under rapid stirring, rigorously purified propylene was pressurized into the flask to reach ∼5−6 atm over 5 min and then slowly released to 1.0 atm over 5 min. This fill-and-release process was repeated five times. The solution was then equilibrated at the desired propylene pressure (1.0−5.0 atm), and the reaction temperature (25 °C) was adjusted using an external water bath. The catalytically active species was freshly generated in 2−4 mL of dry toluene in the glovebox. The catalyst solution was then removed from the glovebox and quickly injected into the rapidly stirred reaction flask using a gastight syringe. The temperature of the reaction mixture during polymerization was monitored in real time using the thermocouple probe. The temperature rise was invariably less than 3 °C during these polymerizations, and the temperature was controlled by occasional addition of ice to the external water bath. After a measured time interval, the reaction was quenched by the addition of 10 mL of methanol. Another 300−400 mL of methanol was then added, and the polymer was collected by filtration, washed with methanol, and dried on the high-vacuum line to a constant weight. Polymerization experiments in 1,3-dichlorobenzene were carried out as described above, but with addition of 50 mL of dry 1,3-dichlorobenzene by cannula through the septum port. Ion-pair complexes were prepared and utilized as described below.

Microstructural Analysis of Polypropylene ^{13}C NMR Spectra. Polymer methyl resonances were assigned according to established criteria[27] and were analyzed at the pentad level. All polymer NMR spectra were collected with identical temperature, solvent, instrument field strength, and acquisition and processing parameters. For systems employing precatalyst **1**, pentad distributions were modeled using the syndiospecific Bernoullian model outlined in Table 16 of ref 38a (p 1316), having probability parameters P_m and P_{mm} of formation for *m* and *mm* stereodefects, respectively. Microstructural analyses of polymers prepared using systems with precatalyst **2** are presented in detail in the Discussion.

***In Situ* Generation of Catalyst Ion-Pairs for Polymerization Studies.** $Me_2C(Cp)(Flu)ZrMe_2$ (**1**) or $Me_2Si(OHF)(CpR^*)ZrMe_2$ (**2**) and the required cocatalyst in a 1:1 ratio were loaded in the glovebox into a vial equipped with a septum, and 2.0−4.0 mL of toluene was added. The mixture was shaken vigorously at room temperature before use.[28] Total amounts used were chosen/refined as required for temperature control and are reported herein (see Tables 1−3).

***In Situ* Activation of $Me_2C(Flu)(Cp)ZrMe_2$ by 1:1 $Ph_3C^+FAl(o\text{-}C_6F_5C_6F_4)_3^-$:$Al(C_6F_5)_3$ for Polymerization.** In the glovebox, $Ph_3C^+FAl(o\text{-}C_6F_5C_6F_4)_3^-$ (**7**, 14.0 mg, 0.010 mmol), $Al(C_6F_5)_3$ (**5**, 5.9 mg, 0.010 mmol), and 8.0 mL of toluene were loaded into a vial, fitted with a septum. This mixture turned orange immediately. The mixture was next shaken at room temperature for 30 min. $Me_2C(Cp)(Flu)ZrMe_2$ (**1**, 4.0 mg, 0.010 mmol) was then added to this orange solution. The mixture was shaken vigorously at room temperature for 20 min before use.

***In Situ* Activation of $Me_2C(Flu)(Cp)ZrMe_2$ by 1:2 Ph_3CCl:$Al(C_6F_5)_3$ for Polymerization.** In the glovebox, $(C_6H_5)_3CCl$ (2.8 mg, 0.010 mmol), $Al(C_6F_5)_3$ (**6**, 11.7 mg, 0.020 mmol), and 4.0 mL of toluene were loaded into a vial, fitted with a septum. This reaction mixture turned orange immediately and was monitored by ^{19}F NMR (C_7H_8, 23 °C): δ −123.015 (m, 6 F, *o*-F), −154.960 (m, 3 F, *p*-F), −163.705 (m, 6 F, *m*-F). $Me_2C(Cp)(Flu)ZrMe_2$ (**1**, 3.9 mg, 0.010 mmol) was then added to this orange solution. The mixture was shaken vigorously at room temperature and injected into the polymerization reactor immediately.

***In Situ* Activation of $Me_2C(Flu)(Cp)ZrMe_2$ by 1:2 Ph_3CCl:$Ga(C_6F_5)_3$ for Polymerization.** In the glovebox, $(C_6H_5)_3CCl$ (2.8 mg, 0.010 mmol), $Ga(C_6F_5)_3$ (**8**, 12.0 mg, 0.020 mmol), and 4.0 mL of toluene were loaded into a vial, fitted with a septum. This mixture turned orange immediately. $Me_2C(Cp)(Flu)ZrMe_2$ (**1**, 3.9 mg, 0.010

(21) Obora, Y.; Stern, C. L.; Marks, T. J.; Nickias, P. N. *Organometallics* **1997**, *16*, 2503−2505.
(22) Massey, A. G.; Park, A. J. *J. Organomet. Chem.* **1964**, *2*, 245−250.
(23) This compound was prepared as a toluene adduct; see refs 11b and 11c. ***CAUTION: $Al(C_6F_5)_3$ has been reported to detonate on attempted sublimation at elevated temperatures.*** Pohlmann, J. L. W.; Brinckmann, F. E. *Z. Naturforsch. B* **1965**, *20b*, 5. Chambers, R. D. *Organomet. Chem. Rev.* **1966**, *1*, 279.
(24) (a) Chien, J. C. W.; Tsai, W.-M.; Rausch, M. D. *J. Am. Chem. Soc.* **1991**, *113*, 8570−8571. (b) Yang, X.; Stern, C. L.; Marks, T. J. *Organometallics* **1991**, *10*, 840−842. (c) Ewen, J. A.; Elder, M. J. Eur. Pat. Appl. 426637, 1991; *Chem. Abstr.* **1991**, *115*, 136 987c, 136 988d.
(25) (a) Pellecchia, C.; Pappalardo, D.; D'Arco, M.; Zambelli, A. *Macromolecules* **1996**, *29*, 1158. (b) Busico, V.; Cipullo, R.; Corradini, P.; Landriani, L.; Vacatello, M.; Segre, A. L. *Macromolecules* **1995**, *28*, 1887. (c) Miyatake, T.; Miaunuma, K.; Kakugo, M. *Macromol. Symp.* **1993**, *66*, 203. (d) Kakugo, M.; Miyatake, T.; Miaunuma, K. *Stud. Surf. Sci. Catal.* **1990**, *56*, 517. (e) Longo, P.; Grassi, A. *Makromol. Chem.* **1990**, *191*, 2387. (f) Randall, J. C. *J. Polym. Sci., Part B: Polym. Phys.* **1975**, *13*, 889.
(26) At 20 °C, the rate of C_3H_6 absorption is estimated to be 0.029 mol/min in toluene at 1.0 atm of C_3H_6, and propylene mass transfer effects (mass transport coefficient) in the $(2\text{-PhInd})_2ZrCl_2$/MAO system in toluene (100 mL) are observed to be insensitive to the presence of up to 4 g of isotactic PP with a maximum stirring speed of 1460 rpm. See: Lin, S.; Tagge, C. D.; Waymouth, R. M.; Nele, M.; Collins, S.; Pinto, J. C. *J. Am. Chem. Soc.* **2000**, *122*, 11275−11285.
(27) Busico, V.; Cipullo, R.; Monaco, G. R.; Vacatello, M.; Segre, A. L. *Macromolecules* **1997**, *30*, 6251−6263.
(28) For cocatalysts **16**−**18**, the resulting reaction mixture was injected into the polymerization reactor immediately. No activity was observed when the activation time of **1** + **16** was longer than 20 min.

Table 1. Comparison of Propylene Polymerization Results with $Me_2C(Cp)(Flu)ZrMe_2$ (**1**) + the Indicated Cocatalysts at 25 °C under 1.0 atm of Propylene[a]

expt no.	cocatalyst (R = C_6F_5; R′ = $C_{12}F_9$)	amount (μmol)	time (min)	PP (g)	ΔT[c] (°C)	T_m[d] (°C)	$k_{p,apparent}$ (M^{-1} s^{-1})[e]	*rrrr*[f] (%)	P_m (%)	P_{mm} (%)	M_w[g] ($\times 10^3$)	M_w/M_n
1[b]	BR_3 (**3**)	20	40	5.9	1	101.4	3.5	68.5	6.85	1.92	79	1.81
2	$Ph_3C^+FBR_3^-$ (**9**)	10	60	0.87	1	104.5	0.69	69.4	6.72	1.80	81	1.99
3[b]	BR'_3 (**4**)	10	5	2.92	3	130.3	28	82.3	2.41	1.96	101	1.85
4	$Ph_3C^+FBR'_3^-$ (**10**)	20	12	1.39	1	137.6	2.8	82.2	2.40	1.87	94	2.11
5[b]	$Ph_3C^+BR_4^-$ (**6**)	4.8	1.25	0.89	3	130.7	71	82.6	2.39	1.87	112	1.95
6	AlR_3 (**5**)	20	45	0.84	1	139.5	0.45	83.1	2.00	2.14	74	2.2
7	$Ph_3C^+FAlR_3^-$ (**11**)	10	4	1.32	2	142.1	16	86.5	1.70	1.42	138	1.95
8	$Ph_3C^+F(AlR_3)_2^-$ (**12**)	1.6	2	0.79	2	143.7	120	85.5	1.90	1.49	147	2.08
9	$(Ph_3C^+)_2F_2(AlR_3)_3^{2-}$ (**13**)	2.5	3	0.99	1	143.5	63	86.3	1.80	1.39	144	1.98
10[b]	$Ph_3C^+FAlR'_3^-$ (**7**)	20	75	5	0.5	145.7	1.6	89.4	0.86	1.52	147	1.85
11	$Ph_3C^+(AlR_3FAlR'_3)^-$ (**14**)	2.6	5	0.94	1	145.8	35	85.1	2.10	1.45	121	1.91
12	GaR_3 (**8**)	20	40	1.3	0.5	138.0	0.78	82.5	2.10	2.13	77	2.85
13	$Ph_3C^+F(GaR_3)_2^-$ (**17**)	10	3	1.17	3	140.5	19	84.3	2.00	1.70	129	1.93
14	$Ph_3C^+ClAlR_3^-$ (**15**)	15	12	0.94	10	139.5	2.5	85.9	1.60	1.76	107	1.86
15	"$Ph_3C^+Cl(AlR_3)_2^-$ "[h]	10	5	1.56	1	139.9	15	85.6	1.70	1.76	127	1.89
16	$Ph_3C^+BrAlR_3^-$ (**16**)	15	60	3.1	0.5	137.9	1.6	85.1	1.60	2.03	126	1.81
17	"$Ph_3C^+Br(AlR_3)_2^-$ "[h]	10	15	1.24	0.5	138.4	3.9	81.4	2.40	2.06	108	1.77

[a] In 54 mL of toluene with precise polymerization temperature control (exotherm <3 °C); estimated [propylene] = 0.83 M for the present conditions, see ref 39. [b] See ref 7. [c] Internal temperature variation (±). [d] Second scan by DSC. [e] Taken as a measure of activity. Determined from polymerization yield, assuming the rate law $v_p = k_p$[catalyst][propylene]; assumes 100% of catalyst metal sites are active. [f] Calculated values from ^{13}C NMR pentad analysis. Complete pentad distributions appear in the Supporting Information. [g] GPC relative to polystyrene standards. [h] Cocatalyst prepared *in situ* with a 1:2 ratio of Ph_3CCl or Ph_3CBr and $Al(C_6F_5)_3$.

mmol) was then added to this orange solution. The mixture was shaken vigorously at room temperature and immediately injected into the polymerization reactor.

Results

The present series of halo(perfluoroaryl)metalate cocatalysts all activate C_s-symmetric complex **1** and C_1-symmetric complex **2** to produce ion-pair complexes that are all active for propylene polymerization. These systems exhibit a broad range of activities and stereoselectivities, with selected cases surpassing previously studied catalyst systems in overall performance, giving strong stereoregulation at high polymerization activities. Results are presented in two parts, the first containing results from experiments using precatalyst **1** and the second giving results from experiments with precatalyst **2**. This is followed by a discussion in which anion-dependent polymerization features across the present collected results are surveyed and discussed in light of what is known from *ex situ* study of these systems,[14] and the remarkable combined high activity and stereoregulation performance of cocatalysts **12** and **14** are considered in detail.

I. Propylene Polymerization Mediated by $Me_2C(Cp)(Flu)ZrMe_2$ (1) Activated with Cocatalysts 5, 8−17, "$Ph_3C^+Cl[Al(C_6F_5)_3]_2^-$ ", and "$Ph_3C^+Br[Al(C_6F_5)_3]_2^-$ ". Active catalyst systems comprised of the archetypal C_s-symmetric precatalyst $Me_2C(Cp)(Flu)ZrMe_2$ (**1**; Cp = C_5H_4, η^5-cyclopentadienyl; Flu = $C_{13}H_8$, η^5-fluorenyl) activated with cocatalysts **5** and **8−17** were investigated in propylene polymerization reactions in toluene solution at 25 °C and at 1.0 atm of propylene, as were systems **1** + "$Ph_3C^+Cl[Al(C_6F_5)_3]_2^-$ " and **1** + "$Ph_3C^+Br[Al(C_6F_5)_3]_2^-$." The results of these experiments are presented in Table 1, along with results previously obtained from parallel experiments using precatalyst **1** activated with **3**, **4**, **6**, and **7**.[7] Additionally, system **1** + $(C_6F_5)_3AlFAl(o\text{-}C_6F_5C_6F_4)_3^-$ (**14**) was investigated in polymerizations carried out in toluene solution under 1.0 atm of propylene, at reaction temperatures spanning the range from −10 to 60 °C, and under 5.0 atm of propylene at 60 °C. These results appear in Table 2.

Across these collected results, polyolefin product polydispersities are consistent with well-defined single-site processes and are rather anion-insensitive. Polymer production rates and product molecular weights are highly anion-sensitive—a marked counteranion dependence of product polymer syndiotacticity and relative *m* and *mm* stereodefect abundance is observed, these new perfluoroaryl cocatalysts uniformly giving enhanced product polymer stereoregularity and exhibiting higher polymerization rates than the corresponding neutrally charged cocatalysts. These anion effects are afforded a detailed treatment in the Discussion section.

As reported previously, the reaction of **1** with cocatalysts **11−13** yields mixtures of species $Me_2C(Cp)(Flu)ZrMe^+FAl(C_6F_5)_3^-$ (**23**) and $\{[Me_2C(Cp)(Flu)ZrMe]_2(\mu\text{-}Me)\}^+[(C_6F_5)_3AlFAl(C_6F_5)_3]^-$ (**24**) in different proportions.[7] These three systems each exhibit similar strong stereoregulation performance (~86% *rrrr*; Table 1, entries 7−9), with activities being high in general but spanning approximately one order of magnitude. Catalyst system **1** + **12** exhibits the highest polymerization activity among the systems discussed here, outperforming even the highly active benchmark system **1** + $Ph_3C^+B(C_6F_5)_4^-$ (**6**). Fluoro-bridged $Ph_3C^+(C_6F_5)_3AlFAl(o\text{-}C_6F_5C_6F_4)_3^-$ (**14**) also affords high syndiospecificity (85.1% *rrrr*, Table 1, entry 11) and heightened polymerization activity.

The fluoro-bridged gallate cocatalyst **17** also produces highly syndiotactic product polymer (84.3% *rrrr*, Table 1, entry 13), comparable to results achieved with fluoroaluminates **11−13**, and exhibits both considerably higher polymerization activity and greater stereoregulation than neutral $Ga(C_6F_5)_3$ (**8**; Table 1, entries 12 and 13).[29] Importantly, all of these new fluorometalate cocatalysts (**10−17**) yield higher product syndiotacticities than do the corresponding neutral cocatalysts **4**, **5**, and **8**.

The reaction of **1** with the new chloro- and bromoaluminate reagents **15** and **16** produces complex organozirconium mixtures

(29) Thermal decomposition of the active species may occur at room temperature, as the polymerization activity decreases dramatically when prolonged activation times are used in the reaction of **1** with **17**.

Table 2. Propylene Polymerization Results with $Me_2C(Cp)(Flu)ZrMe_2$ (**1**) + the Indicated Cocatalysts[a]

expt no.	cocatalyst (R = C_6F_5; R′ = $C_{12}F_9$)	amount (μmol)	temp (°C)	$[C_3H_6]$[b]	time (min)	PP (g)	ΔT[c]	T_m[d] (°C)	$k_{p,apparent}$[e] ($M^{-1}\,s^{-1}$)	rrrr[f] (%)	P_m (%)	P_{mm} (%)	M_w[g] ($\times 10^3$)	M_w/M_n
1	$Ph_3C^+[R_3Al\ FAlR'_3]^-$ (**14**)	4.1	−10	2.83	16	0.6	1	158.1	1.3	91.4	0.628	1.29	254	2
2		2.6	0	1.87	4	0.92	0.5	156.5	19	92.3	0.657	1.06	233	1.95
3		2.6	10	1.31	3	0.76	1.5	149.3	29	88.7	1.00	1.60	174	1.99
4		2.6	25	0.83	5	0.94	1	145.8	35	85.0	1.43	2.09	129	1.91
5		3	40	0.56	6	1.33	1	131.5	52	80.0	2.84	2.17	96	1.96
6		2.6	60	0.36	12	0.78	1	97.8	28	63.4	8.00	2.52	69	1.87
7		1.8	60	2.05[h]	2	1.7	2.5	131.8	91	78.4	2.39	2.91	62	2.43
8	$Ph_3C^+FAlR'_3$- (**7**)[i]	20	−10	2.83	180	0.85	n.o.[j]	156.5	0.033	94.2	0.284	0.96	290	1.86
9		20	0	1.87	60	0.54	n.o.	154.5	0.095	93.8	0.273	1.06	242	2.04
10		20	10	1.31	75	1.58	n.o.	151.2	0.32	92.5	0.446	1.19	204	1.96
11		20	25	0.83	75	5.00	n.o.	145.7	1.6	89.4	0.857	1.54	147	1.85
12		20	40	0.56	60	0.51	n.o.	136.0	0.30	83.9	1.77	2.07	104	2.09
13		20	60	0.36	30	0.25	n.o.	n.o.	0.46	70.3	5.43	2.62	66.5	1.95
14		20	60	2.05[h]	30	2.92	2	127.2	0.94	80.6	2.21	2.52	71	1.86

[a] In 54 mL of toluene with precise polymerization temperature control (exotherm <3 °C). [b] Propylene pressure = 1.0 atm unless otherwise indicated, see ref 39. [c] Internal temperature variation (±). [d] Second scan by DSC. [e] Taken as a measure of activity. Determined from polymerization yield, assuming the rate law $v_p = k_p[\text{catalyst}][\text{propylene}]$; assumes 100% of catalyst metal sites are active. [f] Pentad analysis by ^{13}C NMR. Complete pentad distributions appear in the Supporting Information. [g] GPC relative to polystyrene standards. [h] Propylene pressure = 5.0 atm; see ref 7 for temperature corrections. [i] See ref 39. [j] Not observed (ΔT = 0 °C).

from which only decomposition products can be isolated.[14] However, propylene polymerization experiments again give product polymers with higher syndiotacticity (Table 1, entries 14 and 16) than those produced using the neutral cocatalyst analogue **5** (Table 1, entry 6). Note that lower polymerization activities and lower product stereoregularities are observed with haloaluminate cocatalysts **15** and **16** compared to the fluoroaluminate analogue. Also note that metallocene **1** can be similarly activated by the reaction product of TrCl or TrBr with $Al(C_6F_5)_3$ in a 1:2 ratio (**18** and **19**, respectively) and that comparable product syndiotacticities with far greater polymerization activities are achieved (Table 1, entries 15 and 17) in comparison to **1**-based systems activated with isolable cocatalysts **15** and **16**.

The remarkable observed stereocontrol of highly active catalyst system **1** + **14** motivated a survey of the propylene concentration dependence of stereocontrol, activity, and product polymer M_w in these systems. Table 2 presents temperature and [propylene] dependence data for **1** + **14**-mediated polymerizations, along with temperature and [propylene] dependence data for **1** + **7** that we reported previously.[7] As in the earlier studies, **1** + **14** exhibits an expected drop in product molar mass and syndiotacticity with rising polymerization temperature. An increase in the rates of both *m* and, to a lesser extent, *mm* stereodefect production relative to insertion is also observed (*vide infra* for a detailed analysis of polymer stereodefect formation and counteranion effects).

II. Propylene Polymerization Mediated by C_1-Symmetric Me_2Si(CpR*)(octahydrofluorenyl)$ZrMe_2$ (2, R* = (1*R*,2*S*,5*R*)-*trans*-5-methyl-*cis*-2-(2-propyl)cyclohexyl; (−)-menthyl) Activated with Cocatalysts 3, 6, 7, 12, and 14. We extend our investigation of cocatalysts **3**, **6**, **7**, **12**, and **14** here to include their performance as cocatalysts with C_1-symmetric *ansa*-metallocene precatalyst Me_2Si(CpR*)(octahydrofluorenyl)$ZrMe_2$ (**2**, R* = (1*R*,2*S*,5*R*)-*trans*-5-methyl-*cis*-2-(2-propyl)cyclohexyl; (−)-menthyl), known to produce highly isotactic propylene[21] and with which preliminary cocatalyst/counteranion effects were also observed.[30] Catalyst systems comprised of **2** activated with cocatalysts **3**, **7**, **8**, **12**, and **14** were used in propylene polymerization reactions in toluene solution under 1.0 atm of propylene, at 25 and 60 °C, and also in 1,3-dichlorobenzene solution under 1.0 atm of propylene, at 25 °C. Systems **2** + **3**, **2** + **7**, and **2** + **14** were additionaly studied in propylene polymerization reactions in toluene solution under 5.0 atm of propylene at 60 °C. These results are presented in Tables 3 and 4 (see Experimental Section for details and Figure 3 for a graphical representation of polymerization results).

With the exception of **2** + **7** at 25 °C, product polydispersities are consistent with well-defined single-site processes. In these **2**-based systems, multiple possible active species can be envisioned, considering (a) that the precatalyst itself is diastereotopic and (b) that with dinuclear anionic species arising from activation with fluoro-bridged dialuminates **12** and **14**, different fragmentation−reorganization pathways not seen in the isolated catalyst systems[14] may be operative during polymerization. Indeed, the remarkable combined activities and stereoregulation seen using the present polynuclear cocatalysts indicates that these counteranions profoundly affect reaction coordinate energetics in ways that cannot be fully understood on the basis of *ex situ* study of the polymerization-active ion-pair complexes. The observed narrow polymer molar mass polydispersities do indicate that, within a given polymerization experiment, any present active species either exhibit uniform rate ratios for polymerization and chain release or interconvert rapidly with respect to chain release, the latter excluding cation diastereopic interconversion, which is unlikely. Under catalytic conditions, a large variety of slightly to profoundly different forms of active catalyst may arise, complicating the quantitative analysis of polymerization kinetic results. With multiple catalyst species of unknown relative concentrations, lifetimes, and activities, differentiation among competing pathways for insertion, misinsertion ans catalyst-polymeryl rearrangement may be beyond the reach of available metrics. This situation, which is treated in detail in section V in the Discussion below, does not, however, preclude the examination of ion-pairing effects in more general terms: polymerization activities, product M_w values, product isotacticities, and *rr* stereodefect abundances are again highly anion-sensitive. The activities of the **12**- and **14**-based

(30) Giardello, M. A.; Eisen, M. S.; Stern, C. L.; Marks, T. J. *J. Am. Chem. Soc.* **1995**, *117*, 12114−12129.

Table 3. Propylene Polymerization Results with $Me_2Si(OHF)(CpR^*)ZrMe_2$ (**2**) + the Indicated Cocatalysts[a]

expt no.	cocatalyst (R = C_6F_5; R′ = $C_{12}F_9$)	amount (μmol)	temp (°C)	$[C_3H_6]$[b]	time (min)	PP (g)	ΔT[c] (°C)	T_m[d] (°C)	$k_{p,apparent}$[e] ($M^{-1}\,s^{-1}$)	M_w[f] ($\times10^3$)	M_w/M_n	pentad fraction (%)[g] *mmmm*	*mmrr*	*xmrx*
1	$Ph_3C^+[R_3AlFAlR'_3]^-$ (**14**)	20	25	0.83	30	2.583	1	147.9	2.1	14.2	2.65	81.9	4.11	2.34
2	$Ph_3C^+[R_3AlFAlR_3]^-$ (**12**)	15.4	25	0.83	20	0.632	1	145.8	0.98	10.1	2.81	80.2	4.18	2.86
3	$Ph_3C^+BR_4^-$ (**6**)	20	25	0.83	20	2.51	1	144.8	3.0	6.4	2.11	83.1	2.96	3.65
4	BR_3 (**3**)	12.5	25	0.83	240	1.25	1	141.0	0.20	4.0	2.20	79.4	2.56	5.38
5	$Ph_3C^+FAlR'_3^-$ (**7**)	30	25	0.83	240	0.55	0.5	134.0	0.036	16.4	7.82	61.9	8.65	5.82
6	$Ph_3C^+[R_3AlFAlR'_3]^-$ (**14**)	10	60	0.36	60	0.221	1	n.d.[h]	0.40	1.01	1.28	54.9	6.27	9.65
7	$Ph_3C^+[R_3AlFAlR_3]^-$ (**12**)	20	60	0.36	90	0.393	1	n.d.	0.24	0.87	1.25	56.2	5.59	10.6
8	$Ph_3C^+BR_4^-$ (**6**)	20	60	0.36	10	0.617	2	n.d.	3.4	0.87	1.27	61.1	3.77	10.1
9	BR_3 (**3**)	30	60	0.36	45	0.496	1	n.d.	0.40	0.65	1.21	55.6	3.28	13.2
10	$Ph_3C^+FAlR'_3^-$ (**7**)	40	60	0.36	420	0.315	1	n.d.	0.021	1.22	1.41	46.6	8.09	10.4
11	$Ph_3C^+[R_3AlFAlR'_3]^-$ (**14**)	8	60	2.05[i]	30	2.588	1	138.0	2.1	3.41	2.06	77.7	3.52	4.88
12	BR_3 (**3**)	10	60	2.05[i]	30	3.837	1	129.6	2.5	1.44	1.60	69.2	2.95	8.19
13	$Ph_3C^+FAlR'_3^-$ (**7**)	20	60	2.05[i]	180	3.142	1	137.7	0.17	4.59	2.29	69.0	5.22	5.44

[a] In 54 mL of toluene with precise polymerization temperature control (exotherm <3 °C). [b] Propylene pressure = 1.0 atm unless otherwise indicated; see ref 39. [c] Internal temperature variation (±). [d] Second scan by DSC. [e] Taken as a measure of activity. Determined from polymerization yield, assuming the rate law $v_p = k_p$[catalyst][propylene]; assumes 100% of catalyst metal sites are active. [f] GPC relative to polystyrene standards. [g] Pentad analysis by ^{13}C NMR. Complete pentad distributions appear in the Supporting Information. [h] Not determined. [i] Propylene pressure = 5.0 atm; see ref 7 for temperature corrections.

Table 4. Propylene Polymerization Results with $Me_2Si(OHF)(CpR^*)ZrMe_2$ (**2**) + the Indicated Cocatalysts at 25 °C under 1.0 atm of Propylene, with 1,3-Dichlorobenzene as Solvent[a]

expt no.	cocatalyst (R = C_6F_5; R′ = $C_{12}F_9$)	amount (μmol)	time (min)	PP (g)	ΔT[b] (°C)	T_m[c] (°C)	$k_p[C_3H_6]$[d] (s^{-1})	M_w[e] ($\times10^3$)	M_w/M_n	pentad fraction (%)[f] *mmmm*	*mmrr*	*xmrx*
1	$Ph_3C^+[R_3AlFAlR'_3]^-$ (**14**)	10	25	1.186	1	147.5	1.9	14.2	2.65	83.7	3.11	2.86
2	$Ph_3C^+[R_3AlFAlR_3]^-$ (**12**)	5	20	0.7488	1	147.5	3.0	10.1	2.81	85.3	2.67	2.60
3	$Ph_3C^+BR_4^-$ (**6**)	10	10	1.282	2	146.4	5.1	6.4	2.11	83.3	3.01	2.98
4	BR_3 (**3**)	30	6	1.512	2.5	139.3	3.3	4.0	2.20	74.6	3.62	5.33
5	$Ph_3C^+FAlR'_3^-$ (**7**)	20	90	1.899	0.3	145.8	0.42	16.4	7.82	78.5	3.75	3.94

[a] In 50 mL of 1,3-dichlorobenzene + 4 mL of toluene (solvent for injected catalyst solution) with precise polymerization temperature control (exotherm <3 °C). [b] Internal temperature variation (±). [c] Second scan by DSC. [d] Taken as a measure of activity. Determined from polymerization yield, assuming the rate law $v_p = k_p$[catalyst][propylene]; assumes 100% of catalyst metal sites are active. Propylene solubility unknown for present solvent system. [e] GPC relative to polystyrene standards. [f] Pentad analysis by ^{13}C NMR. Complete pentad distributions appear in the Supporting Information.

catalysts are comparable to that of the $B(C_6F_5)_3$ (**3**)-derived catalyst. Cocatalyst $Ph_3C^+B(C_6F_5)_4^-$ (**6**) affords significantly higher activity, in contrast to experiments with metallocene **1** as the precatalyst. Again, the $Ph_3C^+FAl(o\text{-}C_6F_5C_6F_4)_3^-$ (**7**)-activated catalyst system exhibits significantly lower activity. Temperature effects are also observed to be significantly cocatalyst-dependent for the C_1-symmetric **2**-based catalyst systems. As with C_s-symmetric precatalyst **1** with the present cocatalysts, product stereoregularity and product molecular weight decrease with increasing temperature.[31] This effect is most pronounced when cocatalysts **12** and **14** are used. Surprisingly, activity is also seen to decrease with increasing temperature. This may be due to deactivation via thermal decomposition.

With more polar 1,3-dichlorobenzene as the polymerization solvent, product syndiotacticity, as well as *m* and *mm* stereodefects, were indistinguishable for C_s-symmetric **1** + various cocatalyst systems, as reported previously.[7] In the present study, solvent dependence was also examined for polymerizations mediated by C_1-symmetric **2** + cocatalysts **3**, **6**, **7**, **12**, and **14** under 1.0 atm of propylene pressure at 25 °C (Table 4, entries 1−5). As in the case of **1**, compression in the distribution of polymerization activities, product molecular weights, isotacticities, and *rr* stereodefect abundances is observed for the **2**-based catalysts, indicating that polar solvents significantly weaken ion-pairing effects on stereocontrol in this system. System **2** + **7** exhibits the most dramatic increase in activity and isoselectivity, again pointing to an exceptionally strong ion-pairing in this system when dissolved in nonpolar media.

Discussion

The activation of group 4 metallocene dimethyls such as **1** or **2** with cocatalysts/activators **3**−**17** yields highly reactive, moisture- and oxygen-sensitive metallocenium perfluoroarylmetalate complexes (eq 1) that typically exist as 1:1 contact ion-pairs in low-ϵ media, even at catalytically relevant ($<10^{-4}$ M) concentrations.[10,11] The anionic portions of these active catalyst systems are in general both sterically encumbered and highly charge-delocalized, exhibiting a rich variety of differing coordinative tendencies, reactivities, and modes of interaction with the cation and playing a central role in determining the relative rates and stereoselectivities of monomer enchainment, stereodefect-producing catalyst reorganizations, and polymer chain release processes.[2,7] New cocatalysts **9**−**17** (Scheme 1), accessed by combining trityl halides with exceptionally strong perfluoroarylmetalloid Lewis acids, each feature one or more halogen atoms in M−X or M−X−M bonding arrangements, with these metalloid-bound halogen atoms playing a key role in the activation of dimethylzirconocene precatalyst **1** and the

(31) On raising the polymerization temperature, product isotacticity increases for $Me_2C(CpR)(Flu)ZrCl_2$/MAO while it decreases for $Me_2Si(C_5Me_4)(C_5H_3R^*)ZrCl_2$/MAO. This effect depends on the substituent (R = Me, CMe_2, *t*-Butyl). See: (a) Kleinschmidt, R.; Reffke, M.; Fink, G. *Macromol. Rapid Commun.* **1999**, *20*, 284−288. (b) Grisi, F.; Longo, P.; Zambelli, A.; Ewen, J. A. *J. Mol. Catal. A: Chem.* **1999**, *140*, 225−233.

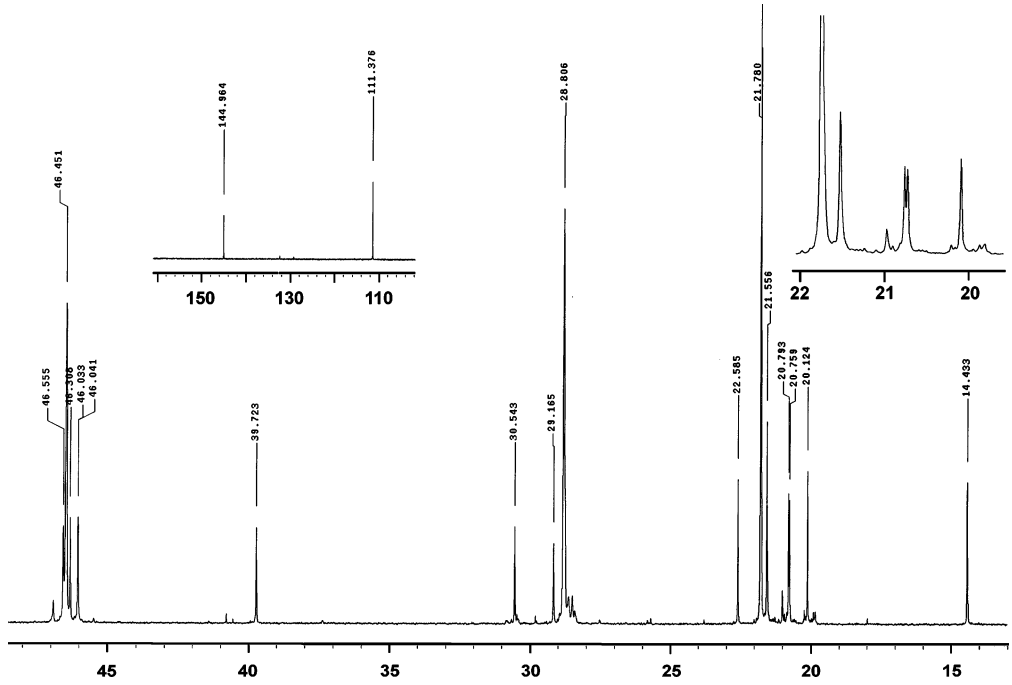

Figure 1. ^{13}C NMR of the isotactic polypropylene generated from $Me_2Si(OHF)(CpR^*)ZrMe_2$ (**2**) + $Ph_3C^+B(C_6F_5)_4^-$ (**6**) under 1.0 atm of propylene at 60 °C in toluene (Table 3, entry 8).

cation−anion interactions of the resulting polymerization-active ion-pair complexes (e.g., **B** below). Details of the syntheses and

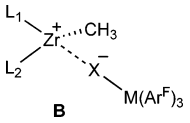

B

the structural and solution characteristics of this new series of cocatalysts/activators, as well as their stoichiometric reaction chemistry with $Me_2C(Cp)(Flu)ZrMe_2$ (**1**) and the products of these activation reactions, are given in ref 14.

The following discussion details the performance characteristics of active catalyst systems derived from reaction of C_s-symmetric metallocene **1** with cocatalysts **3**−**17** as mediators for syndiospecific propylene polymerization, and systems derived from reaction of C_1-symmetric metallocene **2** with cocatalysts **3**, **6**, **7**, **12**, and **14** as mediators for isospecific propylene polymerization. Catalyst system performance is characterized and differentiated herein via the following metrics: (a) polymerization activity, here referring to the rate constant for monomer uptake according to the rate law $v_p = k_p$[catalyst][propylene]; (b) product polymer molar mass distributions, determined by gel permeation chromatography (GPC, also referred to as size exclusion chromatography; see Experimental Section for details); (c) polymer melting temperatures, determined via differential scanning calorimetry (see Experimental Section); and (d) the abundances of specific defects in the otherwise stereoregular polymer backbone, as determined by polymer ^{13}C NMR analysis.

This last polymer microstructural metric, described in detail in several reviews and contributions,[1,32] is extremely powerful for the kinetic analysis of stereocontrol in the production of substantially stereoregular polyolefins. The methine carbon atoms in polypropylene will have either *R* or *S* chirality, and the steric environment experienced by a given methine-bound methyl carbon atom (and thus its ^{13}C NMR chemical shift) will depend on the chirality of the methine carbon to which it is bonded *relative to* the chiralities of its neighbors and, to a lesser degree, its neighbors' neighbors, etc. The polymer backbone can be described as consisting of *racemo* (*r*) and *meso* (*m*) steric dyads (adjacent methine stereocenters having different or equal chirality, respectively), with adjacent steric dyads comprising steric triads *mm*, *mr*, and *rr* (see Schemes 2 and 3 for examples), producing characteristic signals in the methyl resonance region of the polymer ^{13}C NMR spectrum (Figure 1). These triad regions contain fine structure associated with longer stereosequences (*n*-ads) that contain the respective triads, and modern high-field NMR techniques allow resolution of a substantial number of these steric *n*-ad resonances.[27] The observed distribution across the *n*-ad resonance integrals is a function of the probabilities of the various possible insertion and epimerization events, the outcomes of which determine the chiralities of the methine carbons. Modeling of the steric *n*-ad distribution provides a basis for the estimation of the relative probabilities of these events. Several methods[32] have been presented for the modeling of experimental steric *n*-ad distributions via refinement of parameters associated with specific processes thought to occur during propylene polymerization. The most straightforward of these rely on the "stochastic matrix" methodology which can be applied to any catalyst system and generates the probability expressions for all possible steric *n*-ads as a function of parameters of one's choosing.[33]

(32) For recent reviews of propylene insertion, stereoerror production, termination mechanisms, and polypropylene microstructural analysis, see: (a) Resconi, L.; Cavallo, L.; Fait, A.; Piemontesi, F. In ref 1d, pp 1253−1346. (b) Busico, V.; Cipullo, R. *Prog. Polym. Sci.* **2001**, *26*, 443−533. (c) Razavi, A.; Thewalt, U. *Coord. Chem. Rev.* **2006**, *250*, 155−169.

(33) This is an application of the Markov chain method, and the stochastic matrix is sometimes referred to as the "transition matrix". See: Markov, A. A. "Extension of the limit theorems of probability theory to a sum of variables connected in a chain," reprinted in Appendix B of Howard, R. *Dynamic Probabilistic Systems, Volume 1: Markov Chains;* John Wiley and Sons: New York, 1971.

Scheme 2. Syndiospecific Propylene Polymerization and Stereodefect Mechanisms—C_s-Symmetric Precatalyst

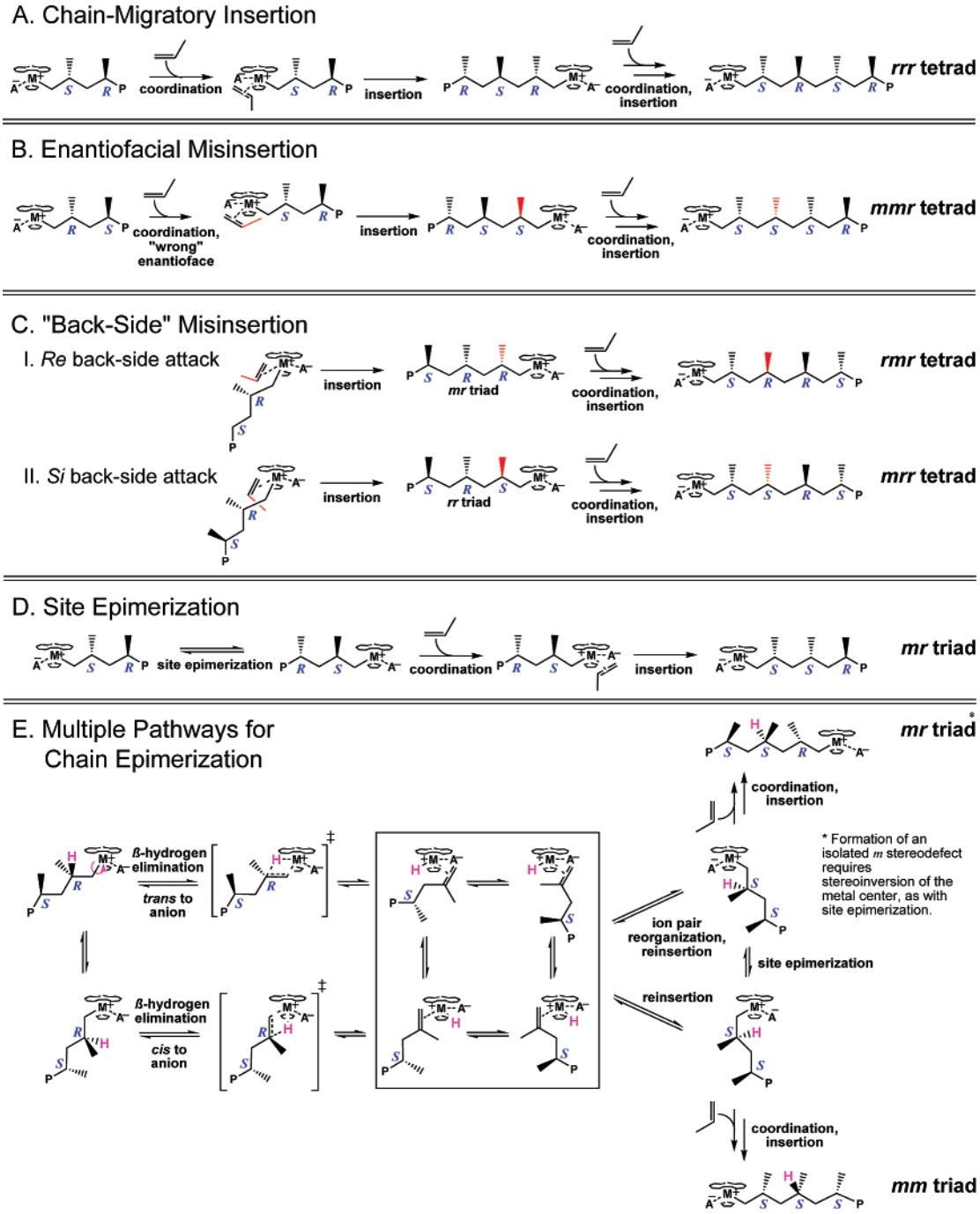

Polypropylenes such as those produced using C_s-symmetric precatalyst **1** + cocatalysts **3**−**17** feature stereosequences consisting substantially of alternating *R* and *S* stereocenters (*r* steric dyads thus predominate) and are termed "syndiotactic". This characteristic alternating pattern is generated via consecutive monomer insertions occurring at alternating faces of the catalyst active site, with stereoselectivities that are equal in magnitude but opposite in sense (Scheme 2A). Occasional errors in this regularly alternating succession ("stereodefects") are generally accepted to arise from a combination of bimolecular monomer misinsertions and unimolecular catalyst−polymeryl stereoinversions ("epimerizations"). The proposed misinsertions include (a) enantiofacial misinsertion−insertion occurring across the "wrong" monomer enantioface (Scheme 2B) and (b) back-side misinsertion−insertion at the "wrong" catalyst enantioface (Scheme 2C). The unimolecular catalyst−polymeryl epimerizations include: (c) site epimerization−stereoinversion of the catalyst metal center without concomitant insertion (Scheme 2D) and (d) chain epimerization−stereoinversion of the polymeryl β carbon atom (Scheme 2E).[32] Histories of these events appear in the form of *m* or *mm* stereodefects in the polymer backbone, thus contributing to the intensity of *m*- or *mm*-containing steric *n*-ads. For a particular syndiotactic polypropylene polymer sample, the distribution across all observed steric *n*-ads can then be modeled via adjustment of parameters representing the likelihood of events that produce *m* or *mm* stereodefects (P_m and P_{mm}, respectively) relative to syndiospecific insertion (which produces *r* steric dyads; see Experimental Section for details

Scheme 3. Isospecific Propylene Polymerization and Stereodefect Mechanisms—C_1-Symmetric Precatalyst

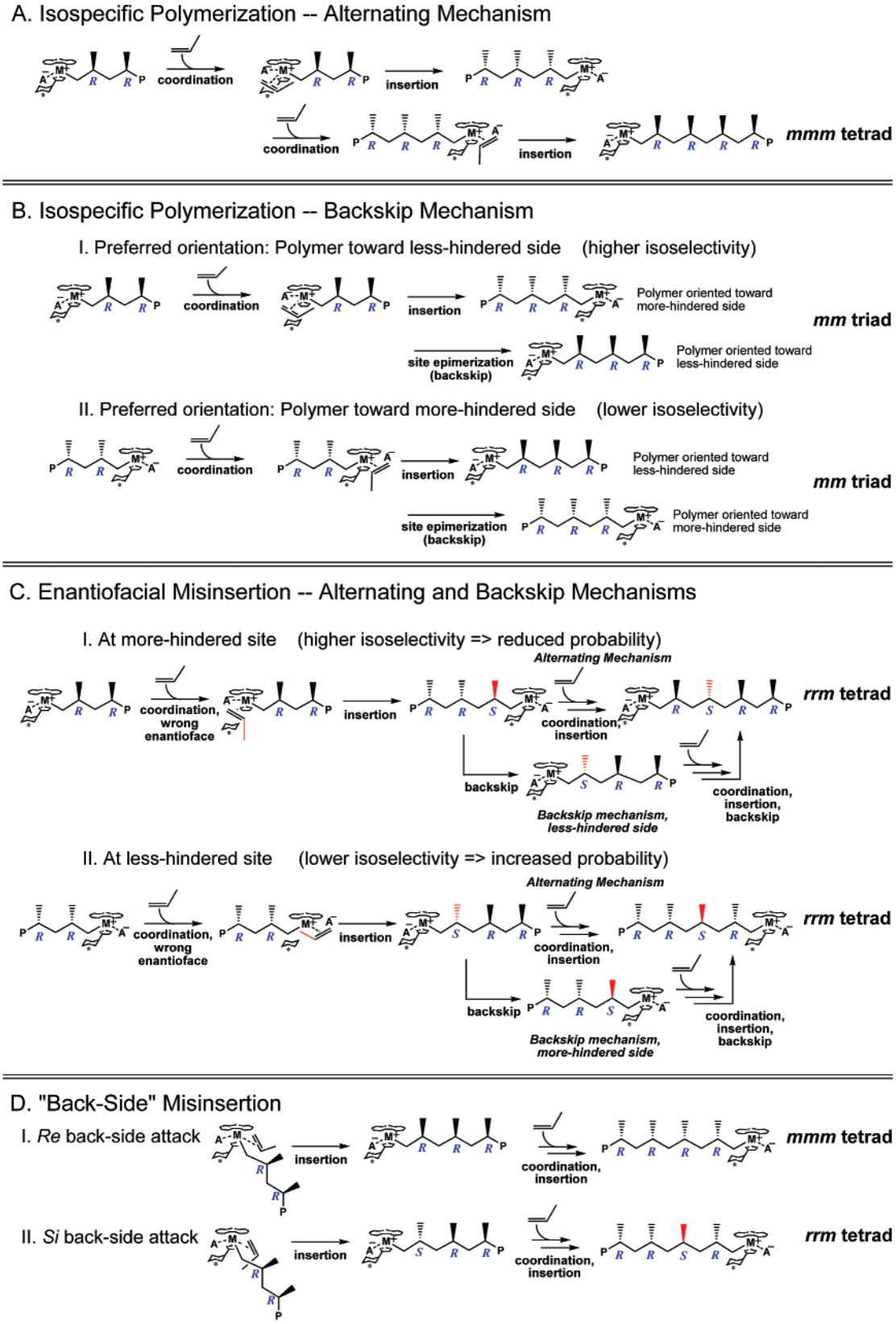

of the parametrization process). The parameter estimates P_m and P_{mm} then constitute key metrics describing the syndioselectivity of the catalyst system. Relative contributions to P_m and P_{mm} from misinsertions vs reorganization processes can be assayed by running series of experiments across which propylene concentration is varied (with all other variables held constant), capitalizing on the differing reaction orders in [propylene] for these processes.[7,26,34]

With metallocene-based catalyst systems employing a C_1-symmetric precatalyst such as $Me_2Si(OHF)(CpR^*)ZrMe_2$ (**2**,

Scheme 3. (Continued)

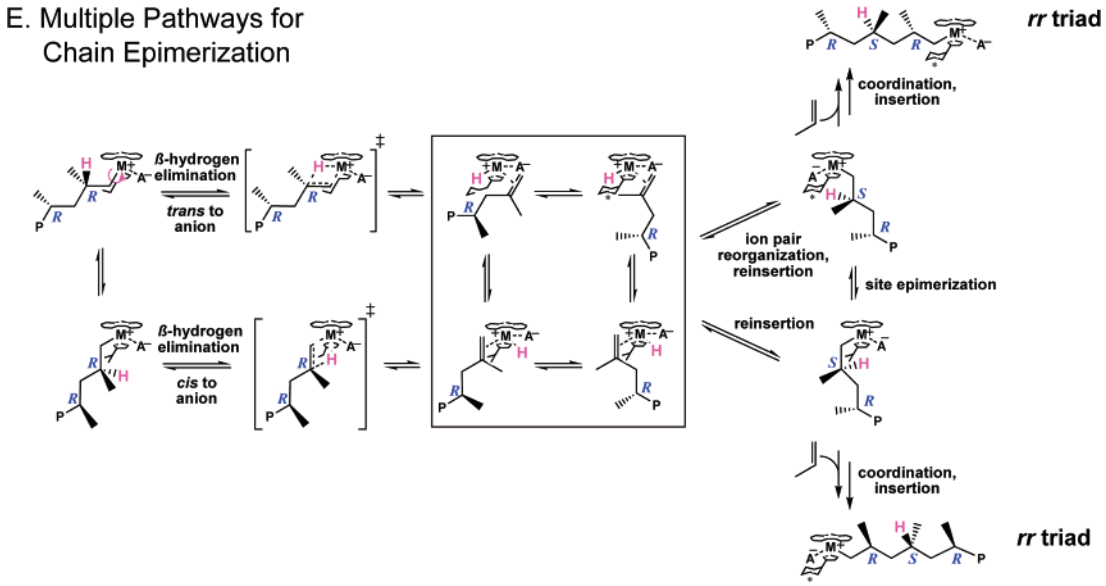

Scheme 1), the structures and thus the enchainment enantioselectivities of the opposing catalyst sides (directions of monomer approach) are unequal. Moreover, the preferred propylene enantioface may be the same at both sides, or it may not, depending on the details of the active catalyst structure and dynamics, as well as the shape of the potential surface associated with the olefin enchainment process.[35] The stereosequences of polypropylenes prepared using metallocene **2** activated with cocatalysts **3**−**17** consist predominantly of *m* dyads (such polypropylenes are termed isotactic). In principle, the same processes that are described above for the C_s-symmetric catalyst case are also possible for C_1-symmetric systems, but with different consequences for the stereosequencing of the polymer backbone (Scheme 3). In the C_1-symmetric case, site epimerization, occurring with different probabilities at the different enantiofaces of the catalyst active site, may be a key factor in determining stereoregularity, since the catalyst faces are *a priori* expected to exhibit different enantioselectivities. However, the proposed rate expressions and microstructural signatures of chain epimerization (Scheme 3E) and site epimerization are indistinguishable from one another, as both processes give rise to changes in *rr* stereodefect abundance, and both have the same reaction order (zero, in this case) in propylene. For the same reason, back-side misinsertion cannot readily be distinguished from enantiofacial misinsertion here (both processes also produce isolated *rr* stereodefects and are putatively first-order in [propylene]; see Scheme 3B,D). Differences in enantioselectivity should, in principle, allow differentiation of site epimerization rates: if, for example, site epimerization (rather than insertion) at the less selective catalyst side can be induced to increase—by an increase in reaction temperature or reduction in monomer concentration—then overall polymer stereoregularity can be expected to increase. However, changes in overall polymer stereoregularity are not as descriptive of mechanistic details as are the abundances of specific stereosequences, the principal difference being in the level of detail. The modeling of steric *n*-ad distributions in isotactic polypropylenes produced using C_1-symmetric precatalysts such as **2** is complicated by the fact that the probabilities for diffrerent insertion and epimerization events depend on which side of the catalyst is employed; this effectively doubles the number of parameters required for accurate description of polymerization stereoselectivity. Moreover, we have found (*vide infra*) that parametrizations in which this property of C_1-symmetric systems is accounted for contain inherent parameteric intercorrelations that seriously compromise the extension of this analytical method to the C_1-symmetric case.

This Discussion is presented in five parts: the first three address catalyst systems derived from C_s-symmetric **1** activated with the present B-, Al-, and Ga-containing species, respectvely, each section beginning with a brief overview of what is known of the structural and solution characteristics and reactivities of each catalyst system, thus setting the stage for a discussion of the nature of the active catalysts under polymerization conditions as manifested in polymerization activities, product polymer molar masses, and product stereoregularities. Al-based system **1** + **14**, yielding a single isolable product ion-pair complex, is unique for its unusual pairing of high activity and excellent stereoregulation performance and is thus afforded a detailed examination, with studies of both reaction temperature and monomer concentration effects. The fourth part of the Discussion extends and generalizes findings on counteranion effects seen in systems employing C_s-symmetric precatalyst **1**, describing polymerization results from C_1-symmetric metallocene **2** activated with cocatalysts **3**, **6**, **7**, **12**, and **14**, and describing the effects of varying monomer concentration and solvent polarity for systems **2** + **3**, **2** + **7**, and **2** + **14**. The fifth section is devoted to the challenge of microstructural analysis for polymers

(34) See, for example: (a) Resconi, L.; Fait, A.; Piemontesi, F.; Colonnesi, M.; Rychlicki, H.; Zeigler, R. *Macromolecules* **1995**, *28*, 6667−6676. (b) Busico, V.; Cipullo, R.; Cutillo, F.; Vacatello, M *Macromolecules* **2002**, *35*, 349−354. (c) Nele, M.; Pinto, J. C.; Mohammed, M.; Collins, S. *J. Polym. Sci., A: Polym. Chem.* **2005**, *43*, 1797−1810. (d) Lahelin, M.; Kokko, E.; Lehmus, P.; Pitkaenen, P.; Loefgren, B.; Seppaelae, J. *Macromol. Chem. Phys.* **2003**, *204*, 1323−1337.

(35) For relevant computational studies, see: (a) Tobisch, S.; Ziegler, T. *Organometallics* **2005**, *24*, 256−265. (b) Tobisch, S.; Ziegler, T. *Organometallics* **2004**, *23*, 4077−4088. (c) Cavallo, L. In *Catalysis by Metal Complexes*; Maseras, F., Lledós, A., Eds.; Computational Modeling of Homogeneous Catalysis 25, Kluwer Academic Publishers: Dordrecht, The Netherlands, 2002; pp 23−56. (d) Jensen, V. R.; Borve, K. J. *J. Comput. Chem.* **1998**, *19*, 947−960. (e) Lanza, G.; Fragala, I. L.; Marks, T. J. *Organometallics* **2002**, *21*, 5594−5612. (f) Lanza, G.; Fragala, I. L.; Marks, T. J. *Organometallics* **2001**, *20*, 4006−4017. (g) Lanza, G.; Fragala, I. L.; Marks, T. J. *J. Am. Chem. Soc.* **2000**, *122*, 12 764−12 777.

produced using C_1-symmetric metallocene-based catalyst systems. Herein, a series of parametrizations based on different sets of mechanistic possibilities is presented, along with the results of application of these models to the present data and a novel numerical method for identifying parametric intercorrelations in these models.

I. Catalyst Systems Derived from $Me_2C(Cp)(Flu)ZrMe_2$ (1), Activated with Trityl Perfluoroaryl Fluoroborates $Ph_3C^+FB(C_6F_5)_3^-$ (9) and $Ph_3C^+FB(o\text{-}C_6F_5C_6F_4)_3^-$ (10). As judged by *in situ* NMR analysis, metallocene $Me_2C(Cp)(Flu)ZrMe_2$ (**1**) reacts readily with cocatalysts **9** and **10**, with methide transfer from the metallocene to the Ph_3C^+ cation and subsequent B−F bond cleavage in both cases. While these chemistries are similar, the soluble reaction products are rather different: **1** + **9** gives $Me_2C(Cp)(Flu)ZrMe^+$ $MeB(C_6F_5)_3^-$ in 30% yield and features an intimate cation−anion contact mediated by the $MeB(C_6F_5)_3^-$ methyl substituent (depicted below; this species is also produced via reaction of **1** with $B(C_6F_5)_3$) in quantitative yield).[7] Yields and reaction stoichiometries for reaction of **1**

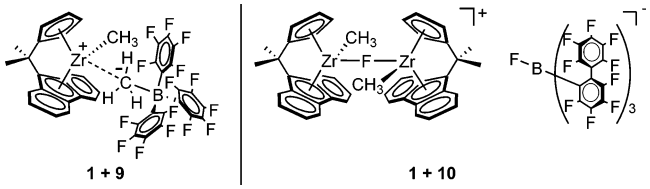

with **9** suggest formation of an insoluble zirconocene fluoride side-product. ^{19}F NMR spectra of the crude reaction mixture in toluene-d_8 give no evidence of persisting B−F or Zr−F linkages. In contrast, system **1** + **10** affords diastereomeric $[Me_2C(Cp)(Flu)ZrMe]_2(\mu\text{-}F)^+FB(o\text{-}C_6F_5C_6F_4)_3^-$, exhibiting no preferred cation−anion contact, together with 1 equiv of free $B(o\text{-}C_6F_5C_6F_4)_3$ present in the crude reaction mixture.

Not surprisingly, polymerization results for system **1** + **9** are quite similar to results with catalyst system **1** + $B(C_6F_5)_3$ (**3**), affording similar polymer melting temperatures, molar mass distributions, and parameter estimates P_m and P_{mm} (see Table 1, entries 1 and 2). On the basis of these results, it appears highly likely that the active catalysts in systems **1** + **9** and **1** + **3** are identical. The difference in activities can be accounted for in light of the comparitively low yield of $Me_2C(Cp)(Flu)ZrMe^+MeB(C_6F_5)_3^-$ in reaction of precatalyst **1** with cocatalyst **9**.

Interestingly, the polymer produced using catalytic system **1** + **10** is also quite similar to that produced using **1** activated with the neutral analogue of cocatalyst **10**, $B(o\text{-}C_6F_5C_6F_4)_3$ (**4**), again with diminished activity (Table 1, entries 3 and 4). While *in situ* NMR monitoring of the reaction of **1** + **10** indicates ultimate formation of $[Me_2C(Cp)(Flu)ZrMe]_2(\mu\text{-}F)^+FB(o\text{-}C_6F_5C_6F_4)_3^-$ [14] together with 1 equiv of **4**, transient μ-methyl-bridged dinuclear diastereomers $[Me_2C(Cp)(Flu)ZrMe]_2(\mu\text{-}Me)^+MeB(o\text{-}C_6F_5C_6F_4)_3^-$ are also observed, being the products of reaction **1** + **4**,[7] and probably arise when free $B(o\text{-}C_6F_5C_6F_4)_3$ is released upon F-ion transfer from **10** to form **21**. The marked similarity in polymerization results between **1** + **10** and **1** + **4** suggests that the active species in these reactions are again the same and that the observed μ-fluoride-bridged dinuclear species (depicted above) has no or extremely low polymerization activity. Another possibility is that, assuming that in this case polymerization proceeds by insertion of propylene into a Zr−C bond and that at least one Zr−F bond remains intact during polymerization, a neutral $Me_2C(Cp)(Flu)ZrMeF$ is close at hand and interacting with the polymerization-active, cationic Zr center as a Lewis base and that the stereoselectivity of this system is similar to that of **1** + **4** by sheer coincidence.

II. Catalyst Systems Derived from C_s-Symmetric $Me_2C(Cp)(Flu)ZrMe_2$ (1), Activated with Trityl Perfluoroaryl Fluoroaluminates $(Ph_3C^+)_xF_x[Al(C_6F_5)_3]_y^{x-}$ (x = 1, y = 1, 11; x = 1, y = 2, 12; x = 2, y = 3, 13), $Ph_3C^+(C_6F_5)_3AlFAl(o\text{-}C_6F_5C_6F_4)_3^-$ (14), $Ph_3C^+XAl(C_6F_5)_3^-$ (X = Cl, 15; X = Br, 16), and "$Ph_3C^+X[Al(C_6F_5)_3]_2^-$" (X = Cl; X = Br). As judged by NMR spectroscopy, metallocene $Me_2C(Cp)(Flu)ZrMe_2$ (**1**) reacts readily with cocatalysts **11**−**13**, accompanied by methide transfer from the metallocene to the Ph_3C^+ cation but without the formal F-ion transfer to Zr observed in the B-based systems. Also, whereas the active catalysts generated using fluoroborates **9** and **10** appear to be the same as those formed with their neutral borane analogues **3** and **4**, this is not the case with the present fluoroaluminate systems.

Activation of **1** with each member of the series $(Ph_3C^+)_xF_x[Al(C_6F_5)_3]_y^{x-}$ (Scheme 1; x = 1, y = 1, **11**; x = 1, y = 2, **12**; x = 2, y = 3, **13**) produces the same two metallocenium ion-pair complexes, mononuclear $Me_2C(Cp)(Flu)ZrMe^+FAl(C_6F_5)_3^-$ (**18**) and dinuclear diastereomeric $[Me_2C(Cp)(Flu)ZrMe]_2(\mu\text{-}Me)^+F[Al(C_6F_5)_3]_2^-$ (**19**), with each system gradually decomposing to pure $Me_2C(Cp)(Flu)ZrMe^+FAl(C_6F_5)_3^-$ (**18**). Their observed

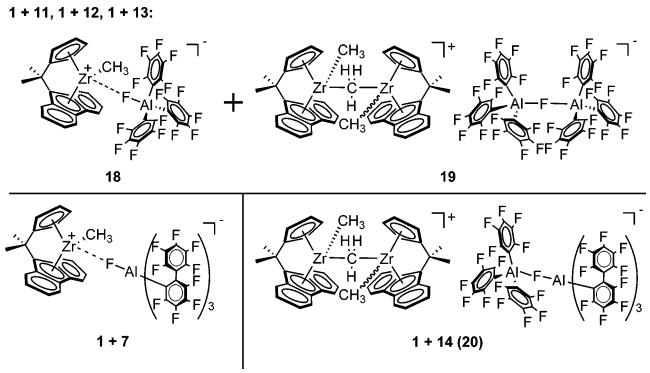

ordering in increasing initial **19**:**18** ratio, **1** + **11** (∼1:1) < **1** + **13** (∼2:3) < **1** + **12** (∼1:2)[14] tracks their orders in increasing activity and diminishing stereoregulation, with product syndiotacticities ranging from 85.5% *rrrr* to 86.5% *rrrr* (Table 1, entries 7−9), arguing (a) that dinuclear species **19** persists during polymerization without decomposing to form species **18**, (b) that trinuclear species **13**, whose activation chemistry resembles that of a 1:1 mixture of **11** and **12**, shows analogous polymerization behavior, and (c) that, while both ion-pairs **18** and **19** are polymerization-active, **19** is more active but probably somewhat less stereoregulating than monomeric **18**. This is in accord with previously observed results:[7] system **1** + mononuclear fluoroaluminate $Ph_3C^+FAl(o\text{-}C_6F_5C_6F_4)_3^-$ (**7**), exhibiting a kinetically inert Zr−F−Al linkage, shows exceptional polymerization stereoregulation but with substantially diminished polymerization activity (Table 1, entry 10), consistent with the hypothesis that, in these systems, direct cation−anion interaction via a μ-fluoro bridge (present in **18** but absent in **19**) significantly attenuates propylene insertion but enhances stereoregulation, suppressing the relative rates vs propagation of both misinsertion and catalyst−polymeryl epimerization pathways.

Asymmetric dinuclear cocatalyst $Ph_3C^+(C_6F_5)_3AlFAl(o\text{-}C_6F_5C_6F_4)_3^-$ (**14**; Scheme 1) activates precatalyst **1** to form stable, diastereomeric $[Me_2C(Cp)(Flu)ZrMe]_2(\mu\text{-}Me)^+(C_6F_5)_3AlFAl(o\text{-}C_6F_5C_6F_4)_3^-$ (**20**), with no formation of a mononuclear analogue observed in an *in situ* NMR study of the activation reaction. Comparison of crystallographic data[13,14] indicates that the anion in active catalyst system **1** + **14** is structurally similar to the anion in the trityl salt cocatalyst **14**, with neither ion-pair exhibiting any specific cation−anion interaction in the solid state. ^{19}F NMR spectroscopic features of these two species are essentially identical, of particular note since, in system **1** + **14**, any direct interaction between the Zr cation and the bridging μ-F moiety is expected to have a profound effect on the ^{19}F NMR chemical shift of the latter.[14] Bridged dinuclear diastereomeric catalyst **1** + **14** (**20**) is highly active for propylene polymerization and exhibits high overall syndiospecificity (85.1% *rrrr*) with low calculated *m* and *mm* stereodefect production parameters (Table 1, entry 11). On the basis of NMR and structural data, this system and species **19** above might be expected to exhibit polymerization activity and stereoregulation characteristics similar to those of **1** + $B(o\text{-}C_6F_5C_6F_4)_3$ (**4**), as both systems feature dinuclear, μ-methyl-bridged cationic fragments together with bulky, apparently noninteracting anions. Comparison of polymerization results from systems **1** + **4** and

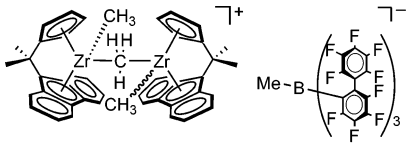

1 + **4**

1 + **14** (Table 1, entries 3 and 11) reveals that, while activities are indeed similar, *rrrr* pentad fractions are different (82.3% for **1** + **4** vs 85.1% for **1** + **14**), with calculated stereodefect probabilities P_m and P_{mm} both elevated in system **1** + **4** (P_m = 2.41% and P_{mm} = 1.96%) compared to system **1** + **14** (P_m = 2.10% and P_{mm} = 1.45%), suggesting a profound differential counteranion effect.

To understand the above results, there are several possibilities to consider. First, one or the other of these systems may actually contain multiple active species, with distributions across species possibly evolving over the course of polymerization. Reactions with such systems often yield polymeric materials having broad or even polymodal molar mass distributions (seen numerically in large polydispersity indices M_w/M_n) or multiple melt endotherms. Importantly, neither catalyst system **1** + **14** nor **1** + **4** exhibits these features, which, while not rigorously proving the presence of uniform catalytically active species, is consistent with and is the generally accepted criterion for a single-catalyst scenario.[1,2] Another possibility is that either **1** + **4** or **1** + **14** undergoes a rapid and complete transformation, yielding a catalyst structure fundamentally different from that observed in *ex situ* studies. In either case, this might involve release of free $Me_2C(Cp)(Flu)ZrMe_2$ upon initiation of polymerization. With **1** + **4**, the presence of excess free $B(o\text{-}C_6F_5C_6F_4)_3$ would then lead to an improvement in activity, as the newly liberated $Me_2C(Cp)(Flu)ZrMe_2$ becomes activated. This, however, is not observed. For **1** + **14**, there are multiple reaction pathways that might be considered: during polymerization, system **1** + **14** could remain (more or less) intact as species **20** or separate into two distinct mononuclear ion-pair complexes, according to eq 2.

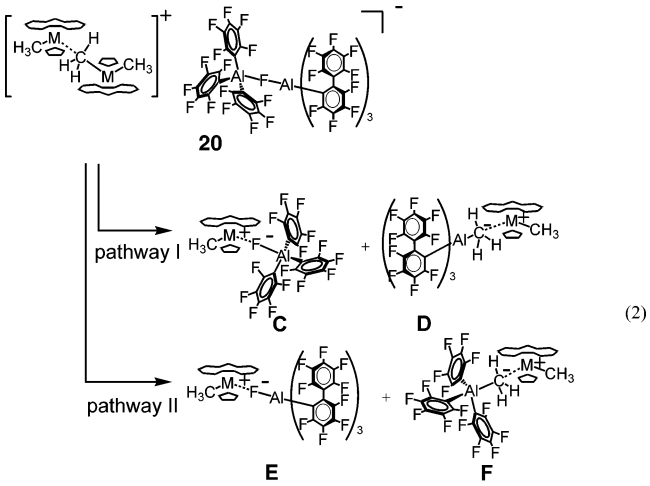

(2)

Let us consider the first pathway of eq 2. In isolation, **1** + **14** does not spontaneously undergo this transformation, possibly reflecting the instability of a neutral $Al(o\text{-}C_6F_5C_6F_4)_3$ fragment (which, in fact, is found to be inisolable);[12b] formation of the C−Al bond of $H_3CAl(o\text{-}C_6F_5C_6F_4)_3^-$ directly via methide transfer from a neutral metallocene dimethyl to the $[(C_6F_5)_3AlFAl(o\text{-}C_6F_5C_6F_4)_3]^-$ anion via an associative process is unlikely as well, considering the significant steric shielding of the Al center outer face by the $o\text{-}C_6F_5C_6F_4$ ligands.[14] Thus, species **D** of pathway I is unlikely. The second pathway is more reasonable in light of the known behaviors of participating systems; species **E** of pathway II is identical to the active species generated in system **1** + **7**, and species **F**, although inisolable, is expected to resemble the reaction product from **1** + $Al(C_6F_5)_3$ (**5**), which produces polypropylene but with marginal activity (Table 1, entry 6). However, the polymerization results are inconsistent with this sequence of events as well. First, catalysts **1** + **7** and **1** + **14** show widely disparate propensities for stereoerror production (**1** + **7** gives P_m = 0.86% and P_{mm} = 1.52% whereas **1** + **14** gives P_m = 2.10% and P_{mm} = 1.45%), and second, system **1** + **14** shows a 20-fold higher activity than system **1** + **7**. These results suggest that the anionic portion of species **20** does not fragment irreversibly during polymerization. It is also conceivable that the $FAl(o\text{-}C_6F_5C_6F_4)_3^-$ moiety remains in intimate contact with $Al(C_6F_5)_3$ *and* impinges upon the active catalyst metal center, in a reversible version of pathway II above, with $Me_2C(Cp)(Flu)ZrMe_2{\cdot}Al(C_6F_5)_3$ acting in an intermediary capacity, or in both modes (eq 3).

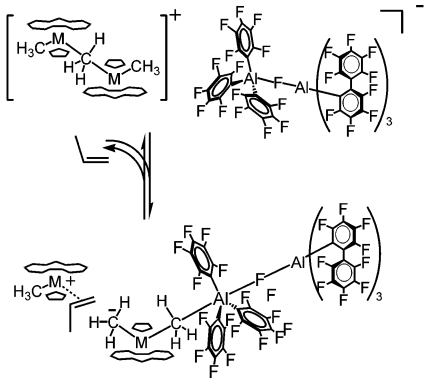

(3)

No spectroscopic evidence for a rearrangement analogous to pathway II in eq 2, nor for the formation of the π-olefin

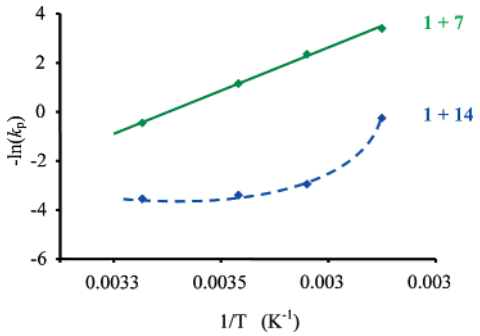

Figure 2. Plots of $-\ln(k_p)$ vs 1/(polymerization temperature) for $Me_2C(Cp)(Flu)ZrMe_2$ (**1**) + cocatalysts $Ph_3C^+FAl(o\text{-}C_6F_5C_6F_4)_3^-$ (**7**) and $Ph_3C^+(C_6F_5)_3AlFAl(o\text{-}C_6F_5C_6F_4)_3^-$ (**14**) under 1.0 atm of propylene over the temperature range from −10 to 25 °C in toluene (Table 2; k_p values corrected for [propylene] temperature dependence).[40] Lines accompanying the data points are presented as a guide to the eye.

complex[36] depicted in eq 3, obtains from *ex situ* studies of isolated **1** + **14**. In any event, it is evident that the $(C_6F_5)_3AlFAl(o\text{-}C_6F_5C_6F_4)_3^-$ anion persists during and is intimately involved in polymerization processes. Moreover, the dependence of propylene insertion rates on reaction temperature indicates that the catalyst system may have access to multiple active modes (*vide infra*).

The remarkable product syndiotacticity and very high polymerization activity observed with C_s-symmetric metallocene precatalyst **1** using fluoro-bridged dinuclear cocatalyst **14** as the activator at 25 °C motivated temperature and [propylene] dependence studies of this system, for comparison with the results on previously characterized catalyst−cocatalyst systems.[7] Table 2 presents temperature and [propylene] dependence data from **1** + **14** polymerizations, along with previously reported temperature and [propylene] dependence data for **1** + **7**, as a basis for comparison.[7] As in the previously studied cases, **1** + **14** exhibits an expected drop in product molar mass and syndiotacticity with rising polymerization temperature. An increase in the probabilities of both *m* and, to a lesser extent, *mm* stereodefect production relative to insertion is also observed. Inspection of Arrhenius plots ($-\ln(k_p)$ vs T^{-1}) for systems **1** + **7** and **1** + **14** (Figure 2) provides added insight into the differences between these two catalytic systems. With **1** + **7**, this plot is linear, as expected for a system in which the rate law is invariant with temperature. This indicates that (a) the catalyst system does not show appreciable temperature-dependent decomposition/deactivation behavior over the temperature range from −10 to 25 °C (erosion of activity is commonly observed at higher temperatures)[1,2,7] and (b) there is only one accessible activation barrier (likely indicating the presence of only one form of active species). However, with catalyst system **1** + **14**, this plot appears to deviate significantly from linearity, indicating that at least one of the above conditions is violated. Our observations with system **1** + **14** indicate that, with the exception of reactions carried out at 60 °C, propylene consumption rates remain constant over the course of polymerization, suggesting that the first condition stated above is not violated. The latter condition could be violated if the catalyst system produces multiple noninteracting active species; however, at all reaction temperatures we observe monomodal polymer molar mass distributions having polydispersities ($M_w/M_n \approx 2.0$) consistent with a single, nonliving catalyst (Table 2). Another possibility is that multiple insertion pathways are available, the relative contributions of which are temperature-dependent. This scenario is consistent with a complex catalytic system exhibiting multiple possible modes of cation−anion interaction. Although the data do not favor any specific interpretation of how this might be manifested, one possibility is that an equilibrium following pathway II (eq 2 above) is operative, with a temperature dependence in equilibrium position.

Increasing the propylene concentration is known to increase the rates of [propylene]-dependent processes vs those of competing unimolecular processes,[37] the effect being greater in systems where unimolecular processes are more facile. Thus, for example, [propylene]-dependent monomer insertion is enhanced vs unimolecular site epimerization,[38] reducing *m* stereodefect abundance and increasing the *rrrr* pentad fraction, while chain release via polymeryl transfer to propylene is enhanced vs chain release via unimolecular β-hydrogen elimination, lowering M_w inasmuch as β-hydrogen elimination is significant. In the present work, the rates of each of these individual processes are significantly and systematically dependent on cation−anion pairing in the catalyst ion-pair complex, making [propylene] dependence experiments an important tool in understanding ion-pairing effects in single-site olefin polymerization systems. The present studies of the [propylene] dependence of stereodefect production using precatalyst **1** and various cocatalysts reveal that (a) increased propylene concentrations are generally accompanied by increases in syndiotacticity and (b) decreases in *m* stereodefect abundance with corresponding increasing propylene concentration are greater with anions believed to be more weakly coordinating, such as $B(C_6F_5)_4^-$ and $MeB(o\text{-}C_6F_5C_6F_4)_3^-$, suggesting that site epimerization in these systems is in general faster.[7] With increased monomer concentrations (0.36 → 2.05 M, see Table 2),[39] catalyst system **1** + **14** evidences a substantial decrease in the probability of *m* stereodefect production vs insertion (P_m) and a slight increase in the probability of *mm* stereodefect production (P_{mm}), with a net increase in total *rrrr* pentad content (63.4 → 78.4% *rrrr*, entries 6 and 7). These increases in *rrrr* pentad content are larger than those observed for catalyst system **1** + $Ph_3C^+FAl(o\text{-}C_6F_5C_6F_4)_3^-$ (**7**; 70.3 → 80.6%) but less than the dramatic increase observed for catalyst system **1** + $Ph_3C^+B(C_6F_5)_4^-$ (**6**; 50.5 → 70.2%).[40] These results indicate that for **1** + **14**, as with **1** + **7**, *m* stereodefect production is largely due to unimolecular site epimerization (Scheme 2D) but that the *mm* stereodefects arise principally from bimolecular enantiofacial misinsertion (Scheme 2B). Since from these results it appears likely that multiple catalytic modes are operative with the **1** + **14** catalyst system, accurate estimates of rate parameters

(36) (a) Stoebenau, E. J., III; Jordan, R. F. *J. Am. Chem. Soc.* **2003**, *125*, 3222−3223. (b) Casey, C. P.; Carpenetti, D. W., II. *Organometallics* **2000**, *19*, 3970−3977. (c) Casey, C. P.; Fisher, J. J. *Inorg. Chim. Acta* **1998**, *270*, 5−7. (d) Casey, C. P.; Hallenbeck, S. L.; Pollock, D. W.; Landis, C. R. *J. Am. Chem. Soc.* **1995**, *117*, 9770−9771.

(37) (a) Resconi, L.; Cavallo, L.; Fait, A.; Piemontesi, F. *Chem. Rev.* **2000**, *100*, 1253−1345. (b) Coates, G. W. *Chem. Rev.* **2000**, *100*, 1223−1252. (c) Veghini, D.; Henling, L. M.; Burkhardt, T. J.; Bercaw, J. E. *J. Am. Chem. Soc.* **1999**, *121*, 564−573. (d) Ewen, J. A.; Jones, R. L.; Razavi, A.; Ferrara, J. D. *J. Am. Chem. Soc.* **1988**, *110*, 6255−6256.

(38) Site epimerization, a stereoinversion at Zr without concomitant propylene insertion, introduces isolated *m* stereodefects in the polymer backbone and is zero-order in [propylene]; see refs 7 and 37.

(39) An empirical model for calculation of solution-phase composition of propylene solutions in toluene and isododecane under relevant conditions is presented in Dariva, C.; Lovisi, H.; Santa, Mariac, L. C.; Coutinho, F. M. B.; Oliveira, J. V.; Pinto, J. C. *Can. J. Chem. Eng.* **2003**, *81*, 147−152.

(40) See entries 16 and 20 of Table 8 in ref 7.

for these processes are inaccessible for individual catalytically active species. In contrast to previously studied systems, increases in product molecular weight are not significant with **1** + **14**, arguing that [propylene]-dependent termination (*β*-hydrogen transfer to propylene) is significant in comparison with unimolecular termination.[41]

In chemistry analogous to the synthesis of species $Ph_3C^+FAl(C_6F_5)_3^-$ (**11**), isolable trityl tris(perfluorophenyl) chloro- or bromoaluminates $Ph_3C^+XAl(C_6F_5)_3^-$ (Scheme 1, X = Cl, **15**; X = Br, **16**) are accessible via reaction of trityl chloride or trityl bromide with $Al(C_6F_5)_3$ (**5**) in 1:1 ratio. Haloaluminates **15** and **16** react rapidly with metallocene $Me_2C(Cp)(Flu)ZrMe_2$ (**1**), forming complex mixtures that, upon attempted purification, yielded only decomposition products $Me_2C(Cp)(Flu)ZrCl(C_6F_5)$ (from **1** + **15**) and $[Me_2C(Cp)(Flu)Zr(\mu_2\text{-}Br)]_2^{2+}\{Al(C_6F_5)_4^-\}_2$ (from **1** + **16**).[14] The crude mixtures from these reactions are,

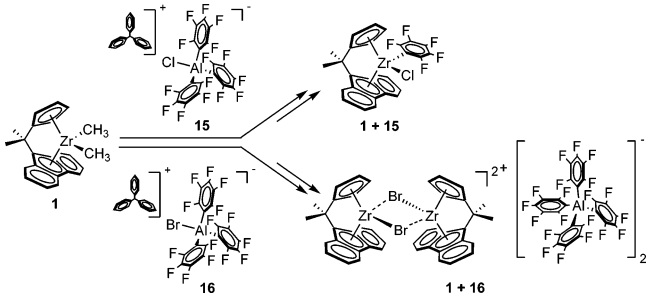

however, moderately active for propylene polymerization (Table 1, entries 14 and 16). Whereas dinuclear fluoroaluminate cocatalyst $Ph_3C^+F[Al(C_6F_5)_3]_2^-$ (**12**) is also isolable, the chloro and bromo analogues are not; however, preparations containing either trityl chloride or trityl bromide and **5** in 1:2 ratio do activate metallocene precatalyst **1** to afford polymerization-active catalyst systems (Table 1, entries 15 and 17). Interestingly, catalyst systems using the putative dinuclear haloaluminates are significantly more active than those of their mononuclear analogues. Comparison of product polymers across this series reveals that, while the active catalyst operating in **1** + $Ph_3C^+ClAl(C_6F_5)_3^-$ (**15**) may be substantially similar to its dinuclear analogue, this does not appear to be the case with **1** + $Ph_3C^+ClAl(C_6F_5)_3^-$ (**16**), the dinuclear analogue here affording reduced stereoselectivity. These polymerization results, together with previously reported NMR, structural, and reactivity studies,[13,14] indicate that the chloro- and bromoaluminate anions are significantly less stable with respect to halide ion transfer to Zr than are the fluoroaluminates.

III. Catalyst System Derived from C_s-Symmetric $Me_2C(Cp)(Flu)ZrMe_2$ (1), Activated with Trityl Perfluoroaryl Fluorogallate $Ph_3C^+F[Ga(C_6F_5)_3]_2^-$ (17). Isolable trityl fluorobis[tris(perfluorophenyl)gallate] ($Ph_3C^+F[Ga(C_6F_5)_3]_2^-$, **17**) is accessible via reaction of trityl fluoride with *in situ*-generated $Ga(C_6F_5)_3$ (**8**). Activation of metallocene $Me_2C(Cp)(Flu)ZrMe_2$ (**1**) with both dinuclear **17** and neutral analogue **8** yield multiple unidentifiable, inisolable species, as reported previously.[14] Nonetheless, these mixtures are active for propylene polymerization (Table 1, entries 12 and 13). Catalyst system **1** + **17** gives a highly syndiotactic product, comparable with results achieved with fluoroaluminates **11**−**13**, and exhibits both polymerization

(41) Liu, Z.; Somsook, E.; White, C. B.; Rosaaen, K. A.; Landis, C. R. *J. Am. Chem. Soc.* **2001**, *123*, 11193−11207.

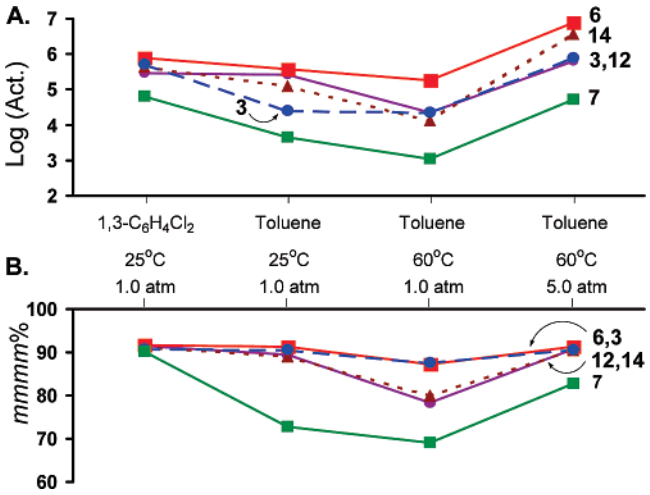

Figure 3. (A) Polymerization activity as a function of solvent, temperature, and propylene pressure. (B) *mmmm* (%) data for polypropylenes produced by C_1-symmetric metallocene $Me_2Si(OHF)(CpR^*)ZrMe_2$ (**2**) + the indicated cocatalysts (labeling defined in Scheme 1) under the specified polymerization conditions.

activity and syndioselectivity that are superior to those of system **1** + $Ga(C_6F_5)_3$ (**8**; Table 1, entries 12 and 13).[29]

IV. Propylene Polymerization Mediated by C_1-Symmetric $Me_2Si(CpR^*)(octahydrofluorenyl)ZrMe_2$ (2, R* = (1*R*,2*S*,5*R*)-*trans*-5-Methyl-*cis*-2-(2-propyl)cyclohexyl; (−)-menthyl), Activated with Cocatalysts 3, 6, 7, 12, and 14. Systematic counteranion effects are readily apparent in catalyst systems using C_s-symmetric metallocene precatalyst $Me_2C(Cp)(Flu)ZrMe_2$ (**1**) and the present family of cocatalyst/activators. We sought to assess the scope and generality of these cocatalyst/activator effects by examining catalyst systems derived from C_1-symmetric precatalyst $Me_2Si(OHF)(CpR^*)ZrMe_2$, known to mediate isospecific proplyene polymerization,[21] activated using cocatalysts $B(C_6F_5)_3$ (**3**), $Ph_3C^+B(C_6F_5)_4^-$ (**6**), $Ph_3C^+FAl(o\text{-}C_6F_5C_6F_4)_3^-$ (**7**), $Ph_3C^+F[Al(C_6F_5)_3]_2^-$ (**12**), and $Ph_3C^+(C_6F_5)_3AlFAl(o\text{-}C_6F_5C_6F_4)_3^-$ (**14**; see Scheme 1 for chemical structures). To parallel prior studies using precatalyst **1**,[7] we have surveyed the effects of reaction temperature, monomer concentration, and solvent polarity. The collected results are presented in Tables 3 and 4, and graphically in Figure 3. Again, the metrics employed for evaluation of polymerization results include activity, polymer molar mass distributions and melting temperatures, and polymer microstructural analysis. A brief synopsis of the latter technique appears in the introductory paragraphs to this Discussion; here we mention that systems using a C_1-symmetric metallocene precatalyst present special complexities in this endeavor. These considerations are discussed in detail following examination of reaction temperature, monomer concentration, and solvent effects on the polymerization process.

Reaction temperature effects were surveyed for systems **2** + **3**, **2** + **6**, **2** + **7**, **2** + **12**, and **2** + **14**, with experiments at 25 and 60 °C (Table 3). For each system, decreases in polymer molar mass and stereoregularity are observed with increasing temperature, with increases in the abundances of *rr* and isolated *r* stereodefects observed in all systems except catalyst **2** + **7**. Systems derived from (perfluoroaryl)fluoroaluminate cocatalysts **7**, **12** ,and **14** (Scheme 1) exhibit decreases in polymerization activity, whereas (perfluoroaryl)borate systems **2** + **3** and **2** + **6** do not. We ascribe this difference to decreased thermal stability

in the fluoroarylaluminate compared to the borate systems. Even in these systems, however, increases in activity with increasing temperature are moderate at best, substantially below the increases predicted from standard Arrhenius behavior, indicating that thermal decomposition is significant for these systems as well.

Mechanistic details of the **2**-based catalyst systems are probed here by studying the effect of changing propylene concentration on the product polymer characteristics. An initial survey of [propylene] dependence trends for systems **2** + **3**, **2** + **7**, and **2** + **14** reveals strong anion dependence both in overall stereoselectivities and in the observed changes in overall stereoselectivity with changing [propylene]. In particular, as [propylene] is increased from 0.36 to 2.05 M, the reduction in *mmrr* pentad fraction is greatest in system **2** + **14** (∼44%; Table 3, entries 6 and 11), less in system **2** + **7** (∼35%; Table 3, entries 6 and 11), and, interestingly, least in system **2** + **3** (∼10%; Table 3, entries 9 and 12). Interpretation of these trends requires a thorough examination of possible insertion and stereodefect production pathways.

Activation of a C_1-symmetric precatalyst with a non-prochiral cocatalyst will, in principle, generate diastereomeric ion-pair complexes, present in different amounts and possibly having quite different polymerization stereoselectivities and activities (eq 4). Some Lewis-basic substituent(s) can be expected to

(4)

preferentially occupy the coordination vacancy adjacent to the electrophilic cation's polymeryl substituent. This could be the counteranion itself, a neutral metallocene (possibly having a methyl, hydrido, or in select cases a halide substituent carrying substantial electron density), a solvent molecule, or a propylene molecule.[36,42]This moiety will provide steric bulk that differs from the polymeryl substituent, thus rendering one epimer thermodynamically distinct from the other (**G** vs **H**). Also, the

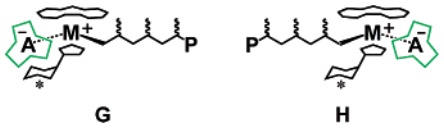

identity of this substituent may change during polymerization. For example, an anionic fragment might be partially or fully displaced by incoming monomer;[35] subsequent chain-migratory insertion may then occur, with the anion taking up the coordination site recently vacated by the polymeryl (following the "alternating" mechanism, Scheme 3A). Conversely, a chain-migratory insertion might be followed by non-insertive site epimerization to regenerate the original, more stable epimer ("backskip" mechanism, Scheme 3B). Distinguishing between these pathways is highly desirable from the standpoint of understanding key structure−function relationships in stereoselection behavior.[43] Both of the above pathways are, in principle, available, their relative likelihoods depending on the differences in steric bulk of the polymeryl vs the Lewis base substituent and possibly also the lability of the Lewis base. If insertion is chain-migratory (i.e., if back-side attack leading to nonmigratory insertion is disallowed, see Scheme 3D), the backskip mechanism requires that the anion or Lewis base substituent be sufficiently labile to allow non-insertive site epimerization. Thus, the degree of preference for the backskip over the alternating pathway might be strongly anion-dependent. Significant observed counteranion effects,[2] particularly arising from large differences in the strength of the cation−anion interaction and based on *ex situ* NMR, structural, and polymerization evidence,[7] suggest that the broad diversity of anions generated using cocatalyst species **3**, **6**, **7**, **12**, and **14** (Scheme 1) should provide a sufficient range of cases to test this hypothesis. Cocatalysts **6**, **12**, and **14** are expected to generate anions that interact weakly with the cationic moiety, whereas **3** is expected to yield a more strongly interacting anion, and **7** is expected to produce a system having an extremely strong cation−anion interaction.

A key question arising from the above considerations is whether the polymeryl substituent or the Lewis base/anion preferentially takes up the less sterically hindered side of the catalyst, i.e., the side opposite the pendant R moiety of the Cp ring. This question bears upon the expected effect of monomer concentration changes upon catalyst system stereoregulation. If the backskip pathway is preferred at low propylene concentrations but the alternating pathway is possible, increasing [propylene] should lead to an increase in the relative contribution of the alternating pathway. An increase in polymer stereoregularity is expected if the backskip pathway presents the less stereoselective side for monomer approach, whereas a decrease suggests the opposite situation.[44] Importantly, we observe in all cases that overall stereoregularity increases significantly with increasing monomer concentration (Table 3), this effect being most pronounced in system **2** + $Ph_3C^+FAl(o\text{-}C_6F_5C_6F_4)_3^-$ (**7**), somewhat less so in system **2** + $Ph_3C^+(C_6F_5)_3AlFAl(o\text{-}C_6F_5C_6F_4)_3^-$ (**14**), and least pronounced in system **2** + $B(C_6F_5)_3$ (**3**). Assuming negligible "back-side" misinsertion and chain epimerization (Scheme 3D,E), these observations are consistent with a stereoregulation model in which (a) the polymeryl substituent preferentially occupies the more sterically hindered catalyst side (configuration **H** above), with insertion occurring at the less-hindered side (configuration **G** above), and (b) the backskip mechanism is favored at lower propylene concentrations, giving way to the alternating mechanism as propylene concentration is increased. The degree of increase in stereoregulation can depend on the degree to which the backskip mechanism is favored at low [propylene] but *also* on the inherent difference in stereoselectivities between the two catalyst sides,

(42) The "anion" in this case may be a stereochemically dynamic species, possibly even incorporating a coordinated dimethylmetallocene moiety; see eq 3 above.

(43) Miller, S. A.; Bercaw, J. E. *Organometallics* **2006**, *25*, 3576−3592.

(44) Indeed, an increase in stereoselectivity with increased [propylene] is consistent with a scenario wherein any [propylene]-independent stereodefect processes are significant, including chain epimerization (Scheme 3E). Studies of chain epimerization in C_2- and C_1-symmetric systems generally require forcing conditions (low monomer concentration, high temperature, or both). See: Yoder, J. C.; Bercaw, J. E. *J. Amer Chem. Soc.* **2002**, *124*, 2548−2555. Also, with C_s-symmetric zirconocene systems (wherein chain epimerization can be kinetically distinguished from other mechanisms), chain epimerization makes a relatively minor contribution to total stereoerror content. See: Veghini, D.; Henling, L. M.; Burkhardt, T. J.; Bercaw, J. E. *J. Amer. Chem. Soc.* **1999**, *121*, 564−573, and ref 7. The contribution of chain epimerization to stereodefect abundance cannot be readily distinguished from that of competition between the backskip and alternating mechanisms solely on the basis of polypropylene microstructural analysis; however, this is, in principle, possible using D-labeled propylene. See: Yoder, J. C.; Bercaw, J. E. *J. Am. Chem. Soc.* **2002**, *124*, 2548−2555, wherein the chain epimerization mechanism is studied for C_2-symmetric metallocene catalyst systems.

both of which can be expected to be anion-dependent. A large increase in stereoselectivity with increasing [propylene] may then be attributable either to a substantial shift from a backskip to an alternating mechanism with some moderate difference in stereoselectivities between the catalyst sides, or to a moderate shift toward alternating insertion coupled with a substantial difference in stereoselectivity between the catalyst sides. These possibilities cannot be differentiated; however, it is reasonable to conclude that a [propylene] dependence in stereoregulation *does* indicate a shift from the backskip to the alternating mechanism with increasing [propylene].

The backskip mechanism involves a step in which the anionic fragment migrates from one catalyst side to the other. If indeed the anion in system **2** + **7** is strongly bound to the cation as expected, one predicts, on the basis of evidence from system **1** + **7**, that this epimerization will be significantly suppressed.[7] However, the present evidence of [propylene] dependence in stereoregulation with this system leads also to the following conclusion: with the catalyst system in configuration **G** above, overwhelming steric congestion might both significantly inhibit monomer insertion *and* attenuate the cation−anion interaction at the more congested side, permitting (or forcing) a backskip pathway wherein insertion occurs preferentially at the less-hindered and thus less stereoselective catalyst side (Scheme 3B), with increasing [propylene] leading to an increase in alternating insertion and an increase in overall stereoregulation performance. In contrast, the more loosely bound ion-pair complex **2** + **14**, lacking the cation−anion bridging μ-F moiety, should allow insertion at the more hindered side (configuration **G**) but *also* facilitate backskip, again leading to a backskip mechanism that gives way to alternating insertion at elevated [propylene]. These arguments are consistent also with the dramatic observed difference in activity between systems **2** + **7** and **2** + **14**. The observed change in stereoregulation with increasing [propylene] in **2** + **14** may also be attributable in part to an increased propensity for chain epimerization in this system vs **2** + **7**. Chain epimerization likely involves a β-hydrogen elimination step,[43] and β-hydrogen elimination leading to chain termination occurs considerably more rapidly in **2** + **14** than in **2** + **7** (*vide infra* for a discussion of polymer molar mass [propylene] dependence and chain termination mechanisms). The above line of reasoning demonstrates that the results themselves are consistent with a scenario in which ion-pairing strength is different in these two systems, with the *origin* of the observed stereoselectivity [propylene] dependence then being different as well.

The observation of significant [propylene] dependence in product polymer M_ws in **2**-based catalytic systems stands in marked contrast to results obtained using C_s-symmetric precatalyst **1** and other reported C_1-symmetric systems.[2b,7] Further evidence that termination via β-hydrogen elimination is favored in the present cases comes from the ^{1}H NMR end group analysis of the product polymers. The presence of the two major endgroups (*n*-Pr and vinylic, Figure 1) is consistent with chain transfer occurring predominantly, if not exclusively, via β-hydrogen elimination.[32] The absence of detectable isopropyl end groups argues that 2,1 monomer insertion, followed by immediate elimination (shown to be first-order in [propylene]),[41] does not occur to a significant extent (eq 5). Also, whereas polymerization activities are significantly anion-dependent, polymer molar mass values are not. These latter observations

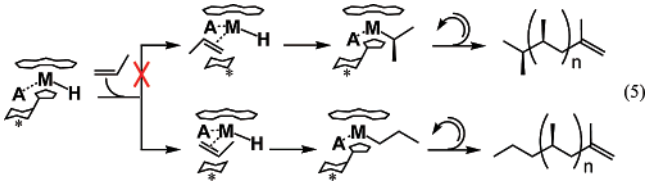

(5)

indicate a pronounced anion dependence in polymer chain release rates, with both insertion *and* chain release occurring significantly more slowly in system system **2** + **7**. This is fully consistent with observations in analogous C_s-symmetric cases (Table 2) and supports the hypothesis that observed differences in polymerization results arise from differences in the binding strength of the FAl(*o*-$C_6F_5C_6F_4)_3^-$ anion to the cation in **2** + **7** by comparison to the anionic moiety in system **2** + **14**.

Replacement of nonpolar toluene (ϵ = 2.38)[45] as reaction medium with a more polar solvent provides a test of the hypothesis that cation−anion interactions are of importance in determining polymerization activity and stereoselectivity, since a more polar solvent such as 1,3-dichlorobenzene (ϵ = 5.02)[44] can be expected to effect separation of the cation and anion during polymerization, attenuating observed counteranion effects. As seen with catalyst systems employing C_s-symmetric $Me_2C(Cp)(Flu)ZrMe_2$ (**1**) with cocatalysts $B(C_6F_5)_3$ (**3**), B(*o*-$C_6F_5C_6F_4)_3$ (**4**), $Ph_3C^+B(C_6F_5)_4^-$ (**6**), and Ph_3C^+FAl(*o*-$C_6F_5C_6F_4)_3^-$ (**7**),[7] counteranion effects are almost completely suppressed for the present systems in which C_1-symmetric precatalyst $Me_2Si(OHF)(CpR^*)ZrMe_2$ is used. We observe a compression in the dispersion of both activities and stereoselectivities across systems **2** + **3**, **2** + **6**, **2** + **7**, **2** + **12**, and **2** + **14** (Table 4, Figure 3).

V. Polymer ^{13}C NMR Microstructural/Mechanistic Analysis of Polypropylenes Produced Using C_1-Symmetric Me_2Si(CpR*)(octahydrofluorenyl)$ZrMe_2$ (2, R* = (1*R*,2*S*,5*R*)-*trans*-5-Methyl-*cis*-2-(2-propyl)cyclohexyl; (−)-menthyl), Activated with Cocatalysts 3, 6, 7, 12, and 14. The above arguments are based on comparison of overall polymer stereoregularities. Differentiation among stereodefect processes according to their proposed rate laws is more challenging with C_1-symmetric catalyst systems than with C_s-symmetric systems. With C_s-symmetric systems, *mm*- and *m*-producing processes can be distinguished quantitatively, whereas with C_1 systems, the analogous processes are each expected to afford either *rr* sterodefects or none at all; thus, they cannot be readily differentiated. Another difficulty is manifested in attempts to model steric pentad distributions using the standard parametric approaches. The primary challenge is that of interparametric correlations, i.e., the tendency for a given parametrization to match the experimental data equally well with different sets of parameter estimates.

In the ensuing paragraphs, we present a generalized stochastic model containing parameters that describe the relative contributions of enantiofacial misinsertion and backskip processes. Using this model as a starting point, we examine a collection of submodels based on reasonable simplifying assumptions. We then present a general method for calculating correlation coefficients among the parameters of any stochastic model,

(45) Wohlfarth, C. In *Landolt-Börnstein, Numerical Data and Functional Relationships in Science and Technology, New Series*; Madelung, O., Ed.; Group IV, Macroscopic and Technical Properties of Matter, Volume 6; Springer-Verlag: Berlin 1991.

taking into account the fact that these regression models are nonlinear in their parameters. Using these tools, we analyze the ^{13}C NMR spectra of the polypropylene samples presented in Tables 3 and 4, generating parameter estimates and correlation matrices for each data set using each model. We analyze the collected results, identifying systematic correlations between the parameters and evaluating each model in terms of its reliability. We then take up a mechanistic question of importance in polymerization stereochemistry: Do the present systems operate under a substantially alternating mechanism or with insertion followed by backskip, or are both pathways operative? The findings that emerge from our correlation analyses shed light on whether or not this question can be meaningfully answered for C_1-symmetric systems solely on the basis of polymer microstructural analysis.

The "stochastic matrix" methodology we employ here can be applied to any catalyst system and conveniently generates the probability expressions for all possible steric *n*-ads as a function of parameters of one's choosing. The basic methodology is described in detail elsewhere,[33,46] so one needs only to present the stochastic matrix itself (often referred to as the transition matrix) to completely describe the chosen statistical model. The columns of this matrix (**A** in conventional notation) are indexed to the possible "states" or outcomes of the present enchainment event, and the rows are indexed (in the same order) to the states of the previous insertion. Reasonably assuming exclusive 1,2 propylene insertion (which places the methyl group of the newly inserted monomer vicinal to the catalyst metal center), these possibilities include *R*(A) and *S*(A), the respective probabilities of *re* and *si* insertions at site A of the catalyst−polymeryl complex, along with *R*(B) and *S*(B) for insertions at site B. The entries a_{ij} of **A** are then probability expressions for an event *j* following event *i*. These probability expressions will be simple functions of the parameters arising from the stochastic model chosen. Matrix **A** can then be used to construct probability expressions for any steric *n*-ad, in the present case, each of the 10 possible pentads. The included probability parameters are then simultaneneously refined until the predicted pentad distribution most closely matches the experimentally determined distribution, using a nonlinear least-squares minimization algorithm.

The basic assumptions implicit in this approach are the following: (i) the polymer can be thought of *both kinetically and structurally* as having infinite length, i.e., that the ratio of terminal and near-terminal methyl resonances to internal methyl resonances in the ^{13}C NMR spectrum is on the order of the spectral S/N ratio or lower (confirmable by determining the olefinic/aliphtic resonance ratios in the ^{1}H NMR, which typically has a much greater S/N ratio); (ii) the probabilities of enantiofacial misinsertion and backskip are not affected by the stereochemistry of the polymeryl stereocenter nearest in the chain to the active site,[47] (iii) the polymer sample is not a mixture of distinct fractions with differing stereoregularities; and (iv) polymerization temperature and monomer concentration are uniform and static during polymerization. To these we add a further assumption, that the rates of 2,1 or 3,1 misinsertions are essentially negligible across the present series of experiments.[43,48] Also, as mentioned above, chain epimerization cannot readily be distinguished from site epimerization solely on the basis of microstructural analysis. As we shall see, however, this is a moot point. The present parametrization is as follows:

parameter	definition
bB	backskip at site B
bA	backskip at site A
rA	*Re* insertion at site A
rB	*Re* insertion at site B

The stochastic matrix **A** arising from this set of parameters is as follows:

$$\mathbf{A} = \begin{array}{c|cccc} & R(\mathrm{A}) & S(\mathrm{A}) & R(\mathrm{B}) & S(\mathrm{B}) \\ \hline R(\mathrm{A}) & \mathrm{bB}\times\mathrm{rA} & \mathrm{bB}\times(1-\mathrm{rA}) & (1-\mathrm{bB})\times\mathrm{rB} & (1-\mathrm{bB})\times(1-\mathrm{rB}) \\ S(\mathrm{A}) & \mathrm{bB}\times\mathrm{rA} & \mathrm{bB}\times(1-\mathrm{rA}) & (1-\mathrm{bB})\times\mathrm{rB} & (1-\mathrm{bB})\times(1-\mathrm{rB}) \\ R(\mathrm{B}) & (1-\mathrm{bA})\times\mathrm{rA} & (1-\mathrm{bA})\times(1-\mathrm{rA}) & \mathrm{bA}\times\mathrm{rB} & \mathrm{bA}\times(1-\mathrm{rB}) \\ S(\mathrm{B}) & (1-\mathrm{bA})\times\mathrm{rA} & (1-\mathrm{bA})\times(1-\mathrm{rA}) & \mathrm{bA}\times\mathrm{rB} & \mathrm{bA}\times(1-\mathrm{rB}) \end{array}$$

The complete set of submodels under consideration is presented in Table 5. Model 1 represents the parametrization arising from matrix **A** with no further assumptions. Model 2, derived from steric arguments and computational studies,[35,49] assumes that the preference of the polymeryl substituent for occupation of one catalyst side over the other (*vide supra* and Scheme 2A) combined with the ease of reorganization—interchanging the more- and less-favored configurations—will lead to a negligible probability of backskip at one side. Models 3 (the alternating mechanism) and 4 (the backskip mechanism) are as described above. These models, by no means novel, have been presented previously in various forms to explore pentad or higher *n*-ad distributions via the stochastic matrix formulation or via other methods.[45,50] Herein we present a systematic evaluation and comparison of all of these models, tested using the present data.

Each of the four models was refined against all 18 sets of experimental pentad distributions appearing in Tables 3 and 4, using a standard nonlinear, quasi-Newton minimization of the

(46) For recent reviews of polypropylene polymerization, stereoerror production, and termination mechanisms and polypropylene microstructural analysis, see: (a) Resconi, L.; Cavallo, L.; Fait, A.; Piemontesi, F. In ref 1d, pp 1253−1346. (b) Busico, V.; Cipullo, R. *Prog. Polym. Sci.* **2001**, *26*, 443−533. (c) Razavi, A.; Thewalt, U. *Coord. Chem. Rev.* **2006**, *250*, 155−169.

(47) For propylene polymerization kinetics, one of the key questions addressable by the stochastic matrix approach is whether stereocontrol is exerted via "site control", i.e., entirely by the catalyst, or via "chain-end control", i.e., by the stereochemistry of the last inserted monomer, see: (a) Hagihara, H.; Shiono, T.; Ikeda, T. *Macromolecules* **1997**, *30*, 4783−4785. (b) Venditto, V.; Guerra, G.; Corradini, P.; Fusco, R. *Polymer* **1990**, *31*, 530−537. (c) Ewen, J. A. *J. Am. Chem. Soc.* **1984**, *106*, 6355−6364. (d) Shelden, R. A.; Fueno, T.; Tsunetsugu, T.; Furukawa, J. *J. Polym. Sci., Part B* **1965**, *3*, 23−26. (e) Shelden, R.; Fueno, T.; Furukawa, J. *J. Polym. Sci., Polym. Phys. Ed.* **1969**, *7*, 763−773. (f) Busico, V.; Cipullo, R.; Talarico, G.; Segre, A. L.; Chadwick, J. C. *Macromolecules* **1997**, *30*, 4786−4790. Indeed, insertion stereoselection can be mediated by a combination of site and chain-end control, and parameters representing the propensity for one over the other can be included in the stochastic matrix. Here we forego this interesting but complicating issue.

(48) The following references find regeoerrors to contstitute <0.5 mol% of insertions: (a) Camurati, I.; Nifant'ev, I. E.; Laishevtsev, I. P. *J. Am. Chem. Soc.* **2004**, *126*, 17040−17049. (b) Song, F.; Cannon, R. D.; Bochmann, M. *J. Am. Chem. Soc.* **2003**, *125*, 7641−7653. See also refs 34b,c.

(49) (a) Razavi, A.; Atwood, J. L. *J. Organomet. Chem.* **1996**, *520*, 115−120. (b) Baar, C. R.; Levy, C. J.; Min, E. Y. J.; Henling, L. M.; Day, M. W.; Bercaw, J. E. *J. Am. Chem. Soc.* **2004**, *126*, 8216−8231. (c) Guerra, G.; Cavallo, L.; Moscardi, G.; Vacatello, M.; Corradini, P. *Macromolecules* **1996**, *29*, 4834−4845. (d) Strauch, J. W.; Faure, J.-L.; Bredeau, S.; Wang, C.; Kehr, G.; Froehlich, R.; Luftmann, H.; Erker, G. *J. Am. Chem. Soc.* **2004**, *126*, 2089−2104. (e) Silanes, I.; Ugalde, J. M. *Organometallics* **2005**, *24*, 3233−3246. Also see ref 45c.

(50) Mohammed, M.; Nele, M.; Al-Humydi, A.; Xin, S.; Stapleton, R. A.; Collins, S. *J. Am. Chem. Soc.* **2003**, *125*, 7930−7941.

Table 5. Submodel Descriptions, Assumptions, and Parametrizations for C_1-Symmetric Metallocene-Mediated Propylene Polymerization

model	parameters				description	$\overline{s^2}$
1	bB	bA	rA	rB	possible backskip at both catalyst sides	1.86
2	bB		rA	rB	possible backskip at B but not A	5.34
3			rA	rB	no backskip at either side (alternating mechanism)	8.64
4			rA		inevitable backskip at B (backskip mechanism)	9.13

mean square about regression, $X^2 = \sum_{i=1 \text{ to } p}(\hat{I}_i - I_i)^2$ of estimated ($\hat{I}_i$) vs experimental (I_i) pentad integrals.[51] The reduced mean square, $s^2 = X^2/(n - p)$, gives some indication of the strength of the model in light of its number of degrees of freedom ($n - p$; n is the number of observations, in this case the nine pentad integral regions, and p is the number of parameters). The overall suitability of each model is gauged by (a) systematic comparison of $\overline{s^2}$ (averaged over all data sets, see Table 5) and (b) determination of a correlation matrix via linearization of the model in the vicinity of the parameter estimates, described below.

For any multiparametric least-squares estimation, it is necessary to assess the risk that the parameters may not be truly independent of one another, i.e., that the solution is unique and that the parameter estimates reflect real physical quantities. The present models are *not* linear in the parameters, the transition matrix **A**, and thus the *n*-ad expressions themselves, consisting of polynomials in the parameters $\mathbf{H} = (H_1, ..., H_i, ..., H_p)^T$,[52] and thus it is not possible to evaluate them using traditional means available for multiple linear regression, such as Pearson's *r* test for collinearity, the derivitive variance inflation factor, standard variance−covariance matrices, or the *F* statistic.[53] However, one can still seek correlations: in any model, if two parameters are correlated, changing either of them by the same amount (in the same direction if they are positively correlated, and in opposite directions if they are negatively correlated) will have the same effect on the calculated *n*-ad integral values $\hat{\mathbf{I}}$. The partial derivatives of the model function with respect to each parameter H_i in the vicinity of the final parameter estimate $\hat{H}_i$ can be estimated numerically; pairwise comparison of these estimated partial derivatives then gives us an indication of possible correlations.

Construction of correlation matrix $\hat{\mathbf{C}}$ is accomplished in the following way:[52] letting the model equation for the integral assigned to *n*-ad ξ_u be $I_u = f(\xi_u,\mathbf{H})$, we may estimate a correlation matrix for the parameters **H** by linearizing the model $\mathbf{I} = (I_1, .., I_u, .., I_p)^T$ over all ξ_u in the vicinity of our calculated $\hat{\mathbf{H}}$, the set of least-squares estimates $\hat{H}_i$ for the parameters H_i. For this purpose, a matrix $\hat{\mathbf{G}}$ can be constructed with elements defined as $\hat{g}_{iu} = \partial\hat{I}_u/\partial\hat{H}_i = \partial f(\xi_u,\hat{\mathbf{H}})/\partial\hat{H}_i$. The rows of matrix $\hat{\mathbf{G}}$ are indexed to the *n*-ads, and the columns are indexed to the refinement parameters. Matrix $\hat{\mathbf{G}}^T\hat{\mathbf{G}}$ is a symmetric $p \times p$ matrix having elements *i*,*j* that are large in magnitude when both $\hat{g}_{iu} = \partial f(\xi_u,\hat{\mathbf{H}})/\partial\hat{H}_i$ and $\hat{g}_{ju} = \partial f(\xi_u, \hat{\mathbf{H}})/\partial \hat{H}_j$ are large for the same *u* (or *u*'s). The normalized form $\hat{\mathbf{C}}$ of $(\hat{\mathbf{G}}^T\hat{\mathbf{G}})^{-1}$, with elements $\hat{c}_{ij} = \hat{w}_{ij}/(\hat{w}_{ii}\hat{w}_{jj})^{1/2}$, is the correlation matrix of the parameters **H** estimated at $\hat{\mathbf{H}}$, based on the assumption that $\partial f(\xi_u,\hat{\mathbf{H}})/\partial\hat{H}$ is a good estimate for $\partial f(\xi_u,\mathbf{H})/\partial H_i$. The off-diagonal elements of $\hat{\mathbf{C}}$ range between −1 and 1 and reflect the degree to which a given change in $\hat{\mathbf{I}}$ can be brought about by changing either $\hat{H}_i$ or $\hat{H}_j$ by the same amount (in the same direction if $\hat{c}_{ij}$ is positive, or in opposite directions if $\hat{c}_{ij}$ is negative). For example, if $\hat{c}_{ij}$ is close to 1, then H_i and H_j are, for all intents and purposes, interchangeable.

We do not attempt to explicitly differentiate $f(\xi_u,\mathbf{H})$; in the present case, each $\partial f(\xi_u,\hat{\mathbf{H}})/\partial\hat{H}_i$ is estimated numerically using the central limit method (eq 6),[5454]

$$\partial f(\hat{i}_u,\hat{\mathbf{H}}) = \lim_{x\to 0} \frac{f(\hat{i}_u, (\hat{H}_1, \cdots, \hat{H}_u + x, \cdots, \hat{H}_p)^T) - f(\hat{i}_u,(\hat{H}_1, \cdots. \hat{H}_u - x, \cdots, \hat{H}_p)^T)}{2x} \quad (6)$$

with $x_{new} = 0.1x_{old}$ between consecutive iterations on *x* and the arbitrary convergence criterion $|\Delta\partial f(\xi_u,\hat{\mathbf{H}})/\partial\hat{H}_j| = 1 \times 10^{-5}$ for consecutive iterations. A correlation matrix can be calculated using the above approach for each set of experimental data, for each model under consideration. Correlation matrices calculated for each data set under each model are included in the Supporting Information. If $\hat{c}_{ij}$ is small in magnitude, then pairwise correlation between H_i and H_j can be ruled out. On the other hand, a large value for $\hat{c}_{ij}$ appearing in a given correlation matrix does not constitute proof that H_i and H_j are *systematically* correlated (i.e., correlated for every data set), just that the available data do not permit their discrimination. Systematic correlations can be evaluated by examining the results obtained using several data sets. If, for example, the correlation matrices for a sufficiently large collection of data sets show strong possible correlations distributed within the correlation matrices with no apparent pattern, then any observed large $\hat{c}_{ij}$ values may be coincidental. For each model we can examine the matrices consisting of the average values for $\hat{c}_{ij}$ across all data sets and their standard deviations. The presence of a substantial average $\hat{c}_{ij}$ value *and* a small standard deviation constitutes strong evidence for a systematic correlation. The apparent correlations discussed below arise from fits to *our* data, which has its own idiosyncracies, e.g., large *xmrx* integral values. These parameters might *not* appear correlated when other data collections are used. In many cases, a model will converge such that the calculated pentad integrals do not change with respect to one or more parameters, generating nonsingular and thus non-invertible $\hat{\mathbf{G}}^T\hat{\mathbf{G}}$ matrices for some or all data sets. These models can safely be regarded as unsuitable and are labeled "ill-conditioned" in the H_j for which $\partial f(\xi_u,\hat{\mathbf{H}})/\partial\hat{H}_j = 0$ for all *u* over the data sets in question. We omit these instances in our comparisons of $\overline{s^2}$ values (*vide infra*). Table 5 gives s^2 values for each of the present data sets under each regression model, and Table 6 provides matrices for each model containing the correlation matrix elements $\hat{c}_{ij}$ averaged over all data sets,

(51) The regression anaysis implementation used here is the Solver package available with the standard release of Microsoft Office Excel 2003 (11.6560.6568) SP2.

(52) The following conventions of notation are used: a vector or matrix **Y** of "true" values or random variables has elements Y_i if it is a vector or y_{ij} if it is a matrix. An estimate of **Y** is denoted $\hat{\mathbf{Y}}$ and has elements $\hat{Y}_i$ if it is a vector or $\hat{y}_{ij}$ if it is a matrix. $\mathbf{Y}^T$ is the transpose of **Y**, and $\mathbf{Y}^{-1}$ is the inverse of **Y**.

(53) Draper, N. R.; Smith, H. *Applied Regression Analysis;* Wiley Series in Probability and Mathematical Statistics; John Wiley and Sons, Inc.: New York 1981; pp 458−529.

(54) A description of the central limit theorem and its applications can be found in the following: Tijms, H. *Understanding Probability: Chance Rules in Everyday Life*; Cambridge University Press: Cambridge, 2004.

Table 6. Correlation Matrices for Models 1−3: Means and Standard Deviations across All Data Sets for C_1-Symmetric Metallocene-Mediated Propylene Polymerization[a]

1	bB	bA	rA	rB
bB	1	*0.498*	*0.742*	*0.650*
bA	0.617	1	*0.492*	*0.535*
rA	0.185	0.680	1	*0.741*
rB	-0.368	-0.595	-0.460	1

2	bB	rA	rB
bB	1	*0.122*	*0.122*
rA	0.215	1	*0.000*
rB	-0.215	-1.00	1

3	rA	rB
rA	1	*0.0451*
rB	-0.480	1

[a] The model number appears in the upper left-hand corner of each array. Model 4, having one parameter, is not shown. Elements below the diagonal are mean $\hat{c}_{ij}$ values across all data sets for which the model is well-conditioned. Elements above the diagonal (shown in italics) are the corresponding standard deviations.

together with their standard deviations. Experimental and calculated pentad distributions, along with each correlation matrix, are presented in the Supporting Information.

Model 1 allows backskip at both sides, having $p = 4$. This model is well-conditioned over all data sets. Large $\hat{c}_{ij}$ values are found with many data sets; however, the standard deviations across all data sets for these $\hat{c}_{ij}$ values are also large, suggesting that there is no systematic correlation. This model gives values for s^2 ranging from 0.31 to 7.55, with $\overline{s^2} = 1.85$, the lowest among the four models. In general, this model provides the best fits to experimental data. Interestingly, refined values for bB are largely near 1.0, suggesting that submodel 4 would be suitable as well. Also of note, and more difficult to reconcile with chemical intuition, is that this model also generally gives large values for bA. This suggests a "nonalternating" polymerization mechanism that occasionally switches between catalyst sides A and B; however, this hypothesis does not mesh well with abundant evidence in support of the generally accepted chain-migratory insertion mechanism.[1a,31b] Also troubling is that, under this model, most data sets give rB < 0.5, suggesting catalyst performance that tends toward C_s symmetry rather than C_2 symmetry.

Model 2 represents possible backskip at side B but not at A, having $p = 3$. This model tends to give rA = rB and is thus ill-conditioned in bB. In two illustrative cases, $\partial f(\xi_u,\hat{\mathbf{H}})/\partial$bB was nonzero for some pentads (probably due to rounding effects), revealing the expected perfect negative correlation between rA and rB. A constraint was then added that rA > rB + 0.01 to break the symmetry of the model. However, under this added constraint, the refined bB value was invariably 1.0, and the model became equivalent to model 4 (and was thus ill-conditioned in rB).

Model 3 represents the alternating mechanism, having $p = 2$. This model is well-conditioned for all data sets and gives correlation values $\hat{c}_{ij}$ that are generally near to −0.5, with a quite small standard devation (0.045) indicating a possible systematic partial correlation. Also of note, the difference in enantioselectivity (rA − rB) is small (1−6%) for all data sets. Values for s^2 range from 1.68 to 29.7, with $\overline{s^2} = 8.64$ ranking third best.

Model 4 represents the backskip mechanism, with $p = 1$. This model has only one parameter, rA, and thus has no potential correlations to evaluate. Values for s^2 range from 1.66 to 31.8, with $\overline{s^2} = 9.13$, ranking last among the present models. It is noteworthy that neither this model or model 3 can be said to be more appropriate for the given data (i.e., both appear to perform marginally). However, that model 1 is fairly well-behaved and uniformly gives large values for bB lends credence to this model.

Analysis of the above models constitutes an investigation of whether a distinction between alternating and backskip mechanisms can be made on the basis of ^{13}C NMR polymer microstructural analysis for this particular family of C_1-symmetric catalyst systems. Model 1, allowing backskip at both sides, is well-conditioned and apparently free of systematic correlations. However, it is troubling that this model consistently yields large values for both bB and bA. Comparison of models 3 (the alternating mechanism) and 4 (the backskip mechanism) again is uninformative: model 3 appears to suffer from a fatal systematic correlation, and model 4 has no basis for evaluation other than the s^2 values it produces. From the above results, it becomes clear that (a) even models that produce reasonable fits to experimental data cannot be rigorously relied upon and (b) one model appearing to perform better than another by no means indicates that the kinetic assumptions underlying it are more valid. Conversely, the presence of apparent correlations in a given parametrization does not demonstrate that the underlying stochastic model is without merit, just that microstructural analysis alone cannot be used to support it.

Systematic counteranion effects on the absolute rates of specific polyinsertion and reorganization processes, demonstrated rigorously for systems based on C_s-symmetric precatalyst **1**, are not clearly in evidence for the analogous C_1-symmetric cases. However, it is evident from the above analysis that this is not necessarily due to the absence of such counteranion effects but rather to what can be described as a problem of resolution in the interpretation of polymer microstructural data; i.e., the absence of evidence for counteranion effects does not, in this case, indicate that these effects do not exist. The above analysis can be implemented as described above in any standard spreadsheet application; in the interest of knowing what can and cannot be concluded on the basis of experimental results, the authors invite the polymer chemistry community to take advantage of this nonlinear correlation technique where appropriate for stochastic modeling of polymer microstructural data.

Conclusions

In this contribution we have detailed the propylene polymerization performance of a series of metallocene-based catalyst systems derived from a new family of well-defined, sterically encumbered and charge-delocalized single-molecule cocatalysts combined with archetypal C_s-symmetric precatalyst $Me_2C(Cp)(Flu)ZrMe_2$ (**1**; Cp = C_5H_4, η^5-cyclopentadienyl; Flu = $C_{13}H_8$, η^5-fluorenyl) and C_1-symmetric precatalyst $Me_2Si(OHF)(CpR^*)$-

$ZrMe_2$, (**2**; OHF = $C_{13}H_{16}$, η^5-octahydrofluorenyl; CpR* = η^5-3-(−)-menthylcyclopentadienyl). These catalyst systems are in general thermally robust and in some cases produce highly stereoregular polypropylenes with unprecedented high polymerization activities. The cocatalysts are mononuclear and polynuclear fluoro- to perfluoroarylborate, -aluminate, and -gallate species and represent a broad class of trityl halide adducts of neutral, highly Lewis acidic perfluoroarylmetalloid species. Details of the synthesis, characterization, and activation chemistry of these new cocatalysts have been described in a separate contribution.[14]

As observed in previous cocatalyst studies, observables such as polymer stereoregularity, stereodefect abundances, molar mass, and polymerization activity are all found to be strongly dependent on catalyst−cocatalyst ion-pairing strength, with catalyst systems derived from these new polynuclear perfluoroaryl cocatalysts in general exhibiting greater stereoregulation and polymerization activities than earlier systems employing their neutral analogues. Similar to previous findings, using more polar 1,3-dichlorobenzene as reaction medium, product polymer molar mass, stereoregularity, and activity are found to converge, indicating that ion-pairing plays an important role in determining the relative rates of termination and stereodefect production processes vs termination.

Catalyst species featuring both mononuclear and polynuclear fluoroaluminate counteranions generally exhibit a uniform, strongly reduced proclivity for stereodefect-introducing reorganizations, with those systems observed by *ex situ* spectroscopy to lack a μ-F linkage between the cation and anion affording the greatest polymerization activities, this latter effect being substantial. Our interpretation is that differences in activity arise from the absence of a persistent Al−F−Zr linkage in the polynuclear systems but that, in both mono- and polynuclear systems, the anion is intimately involved in the insertion reaction and confers a strong stereoregulation effect. These cases wherein unprecedented stereocontrol is observed together with very high polymerization activities constitute a significant advance in catalyst system development for stereoselective olefin polymerization. In the most dramatic examples, we observe syndioselectivities (and catalyst thermal stabilities) on par with highly stereoregulating but much less active catalyst systems and polymerization activities similar to very active (and thermally unstable) but poorly stereoregulating catalyst systems.

Findings using C_1-symmetric precatalyst **2** with the present series of cocatalysts support the hypothesis that the presence or absence of a cation−anion bridging moiety (μ-F or μ-Me) significantly affects the relative rates of insertion and competing stereodefect production and termination processes. From [propylene] dependence experiments, enhanced termination via β-hydrogen elimination is observed in systems in which no cation−anion bridging moiety is detected, and attenuated β-hydrogen elimination is observed in systems in which a kinetically inert cation−anion contact does exist. On the basis of these observations, we can differentiate between the contrasting origins for observed similarities in [propylene]-independent stereodefect production rates in these systems: in the bridged $Zr^+\cdots X^-$ systems, suppression of insertion at the more hindered catalyst side leads to formation of *rr* stereodefects via a backskip mechanism that gives way to alternating insertion at elevated [propylene], whereas in the unbridged systems, both backskip (facilitated here by more facile anion migration rather than inhibited insertion) *and* chain epimerization (involving a β-hydrogen elimination step) are likely operative as [propylene]-independent *rr* stereodefect production processes.

The important topic of polypropylene ^{13}C NMR microstructural analysis is examined in the case of polymers produced using a C_1-symmetric metallocene preceatalyst, with a standard parametric model based on a combination of enantiofacial misinsertion and backskip mechanisms and a collection of its submodels, assessed using a precise method for quantifying interparametric correlations. The result is a significantly clearer picture of the advantages and inherent dangers of using the stochastic approach to interpret polymerization results obtained using a C_1-symmetric precatalyst. While this analysis underscores the care that must be taken in interpreting such results, observations on overall stereoregulation and chain release behavior in the present series of polymerization results obtained using C_1-symmetric precatalyst **2** plus the present cocatalysts are consistent with the general hypothesis, previously detailed using C_s-symmetric precatalyst **1**, that ion-pairing strength is of central importance in determining the relative rates of individual insertion, reorganization, stereodefect production, and chain release processes available during metallocene-mediated propylene polymerization.

The unusual combination of high activity and high stereoselectivity observed in catalyst systems formed by combining precatalysts **1** or **2** with new bulky fluoroaryl cocatalysts **12** or **14** may stem, in part, from the presence of an additional, neutral Lewis-basic dimethylmetallocene fragment that outcompetes the bulky, charge-delocalized anion for occupancy of the catalyst's open coordination site. This hypothesis suggests directions for continued improvements in stereospecific olefin polymerization catalyst systems based on further exploration and elucidation of cocatalyst chemistry and kinetics.

Acknowledgment. Financial support by the U.S. Department of Energy (DE-FG02-86ER1351) is gratefully acknowledged. M.-C.C. thanks Dow Chemical for a postdoctoral fellowship, Dr. M. Oishi for helpful discussions, and Dr. P. Nickias of Dow for GPC measurements. C.Z. thanks the Italian CNR for a postdoctoral fellowship, and A.M.S. thanks the University of Jordan for a sabbatical leave. J.A.S.R. thanks Dr. M. Sales of Northwestern University for helpful discussions.

Supporting Information Available: Experimental and calculated pentad distributions, along with correlation matrices for each stochastic model employed. This material is available free of charge via the Internet at http://pubs.acs.org.

JA0680360